View metadata, citation and similar papers at core.ac.uk

brought to you by CORE

provided by UNT Digital Library

LAWRENCE
LIVERMORE
NATIONAL
LABORATORY

UCRL-JRNL-228632

Fossil and Contemporary Fine Carbon Fractions at 12 Rural and Urban Sites in the United States

B. Schichtel, W. Malm, G. Bench, S. Fallon, C. McDade, J. Chow

March 4, 2007

Journal of Geophysical Research - Atmospheres

Disclaimer

This document was prepared as an account of work sponsored by an agency of the United States Government. Neither the United States Government nor the University of California nor any of their employees, makes any warranty, express or implied, or assumes any legal liability or responsibility for the accuracy, completeness, or usefulness of any information, apparatus, product, or process disclosed, or represents that its use would not infringe privately owned rights. Reference herein to any specific commercial product, process, or service by trade name, trademark, manufacturer, or otherwise, does not necessarily constitute or imply its endorsement, recommendation, or favoring by the United States Government or the University of California. The views and opinions of authors expressed herein do not necessarily state or reflect those of the United States Government or the University of California, and shall not be used for advertising or product endorsement purposes.

Fossil and Contemporary Fine Carbon Fractions at 12 Rural and Urban Sites in the United States

Bret A. Schichtel[1], William C. Malm[1], Graham Bench[2], Stewart Fallon[2], Charles E. McDade[3], Judy C. Chow[4]

[1]National Park Service, Atmospheric Science (CIRA), Colorado State University, Fort Collins CO
[2]Center for Accelerator Mass Spectrometry, Lawrence Livermore National Laboratory, Livermore CA
[3]Crocker Nuclear Laboratory, University of California, One Shields Avenue, Davis CA
[4]Desert Research Institute, Reno, NV

Fine particulate matter collected at two urban, four near-urban, and six remote sites throughout the United States were analyzed for total carbon (TC) and $^{14}C/C$. Samples were collected at most sites for both a summer and winter season. The $^{14}C/C$ was used to partition the carbon concentrations into fossil and contemporary fractions. On average, contemporary carbon composed about half of the carbon at the urban, ~70–97% at near-urban, and 82–100% at remote sites. At Phoenix, Arizona, and Seattle, Washington, one monitor was located within the urban center and one outside to assess the urban excess over background concentrations. During the summer, the urban and rural sites had similar contemporary carbon concentrations. However, during the winter the urban sites had more than twice the contemporary carbon measured at the neighboring sites, indicating anthropogenic contributions to the contemporary carbon. The urban fossil carbon was 4–20 times larger than the neighboring rural sites for both seasons. Elemental (EC) and organic carbon (OC) from TOR analysis were available. These and the $^{14}C/C$ data were used to estimate characteristic fossil and contemporary EC/TC ratios for the winter and summer seasons. These ratios were applied to carbon data from the IMPROVE network to estimate the fraction of contemporary carbon at mostly rural sites throughout the United States. In addition, the ratios were used to semiquantitatively estimate the contribution of secondary organic carbon (SOC) to the fossil and contemporary carbon. SOC accounted for more than one-third of the fossil and contemporary carbon.

1. Introduction

Carbonaceous aerosols are a major component of the particulate matter less than 2.5 microns ($PM_{2.5}$) [*Hegg et al.*, 1997; *Malm et al.*, 2004]. In the United States, the annual $PM_{2.5}$ total carbon (TC) concentrations ranges from less than 1 $\mu g/m^3$ in the rural West to 3 $\mu g/m^3$ in the rural Northwest and Southeast, and over 4 $\mu g/m^3$ in many urban centers (Figure 1). Carbon compounds are also the largest component of $PM_{2.5}$ at many rural sites in the western United States and urban centers throughout the United States [*Malm et al*., 2004; *Debell et al.*, 2006], and the carbon mass fraction is increasing as sulfate aerosols continue to decrease [*Malm et al.*, 2002; *Husain et al*., 2004; *Brewer and Adlhoch,* 2005]. The high carbon concentrations and their efficient scattering and absorption of visible and infrared radiation make them a key factor in atmospheric transparency and the balance of solar radiation [*Adams et al.,* 1990; *Malm et al.*, 1994; *Hegg et al*., 1997; *Jacobson,* 2001a, 2001b]. Carbonaceous emissions from wood burning and fossil fuel combustion also have possible health effects [*Lewis et al.*, 1988; *Salvi et al*., 1999].

Carbonaceous aerosols arise from a wide array of sources including combustion of fossil fuels, meat cooking, and biomass burning [*Bond et al*., 2004]. Secondary organic aerosol (SOA) produced from biogenic and combustion volatile organic compounds (VOC) can also be a significant contributor to organic aerosols. The diverse carbon sources and atmospheric processing results in a complex mixture of compounds with widely differing reactivities, volatilities, and other properties, leading to difficulties in sampling and analysis [*Eatough et al*., 1989; *Hering et al.*, 1990; *Rogge et al*., 1993]. This in turn results in an incompletely characterized mixture, complicating the modeling of ambient concentrations and determining the contributions from their sources.

The distinction most commonly drawn within the carbonaceous component is one between elemental (EC) and organic (OC) fractions, based on thermal optical reflectance (TOR) or thermal optical transmission (TOT). These techniques measure the evolution of carbon vapors and changes in sample reflectance or transmittance during a programmed cycle of sample heating and oxidation [*Chow et al*., 1993; *Birch and Cary*, 1996]. Thermal optical methods accurately measure the total carbon (TC) concentrations, but the distinction between OC and EC is operational, depending on the sensitivity to temperature, combustion atmosphere, and the optical method [*Chow et al*., 2001; *Currie et al*., 2002]. These are inexpensive analysis techniques and

are precise at low filter mass loading, making them suitable for routine monitoring networks. A TOR carbon analysis is currently being used in the Interagency Monitoring of Protected Visual Environments (IMPROVE) monitoring network [*Malm et al.*, 1994] to determine the carbon concentrations in 24-h $PM_{2.5}$ samples collected at ~160 monitoring sites in mostly rural and remote areas of the United States (Figure 1). A TOT carbon analysis is being used in the Speciated Trend Network (STN) to determine the carbon concentration in 24-h $PM_{2.5}$ samples at over 250 sites primarily located in urban and suburban settings [*Flanagan et al*., 2006]. The temperature profile used in the STN TOT analysis is different from that used in IMPROVE.

The fraction of EC and OC in the primary emission is source dependent, and OC/EC/TC ratios have been used to infer the contributions of biomass burning, primary urban emissions, and SOA [e.g., *Turpin et al.*, 1991; *Cabada et al*., 2004; *Malm et al*., 2004]. However, there are large variations in the ratios within the same source categories [e.g., *Gillies and Gertler,* 2000], so the results are semiquantitative in nature. One means of refining these results is to combine the carbon thermal profiles with other aerosol properties and constituents in receptor models to estimate the contributions from source types such as mobile sources and biomass burning [*Lewis et al*., 2003; *Kim et al*., 2004]. However, due to collinearities in the data, these results often suffer from large errors and ill-defined source categories.

The source apportionment of the carbon fraction has been improved using specific organic marker species [*Schauer et al*., 1996; *Chow and Watson*, 2002; *Zheng et al*., 2002]. Unique molecules (or molecular tracers) are identified with such approaches for a source, and the relative abundance of these species in the ambient samples are used to deduce fractional contributions from each profiled source. While compound-specific analysis has proven its value in a variety of atmospheric chemistry studies, numerous source profiles are often needed to apportion a significant amount of the ambient aerosols, and the approach often suffers from only being able to characterize ~30% or less of the total organic mass [*Rogge et al.*, 1993]. In addition, organic compounds can be formed or degraded in the atmosphere due to chemical reactions, causing the source profiles to change over time.

An alternative carbon source apportionment technique is based on the content of radiocarbon, ^{14}C, in a sample. Radiocarbon is present at a small but approximately constant level in living (or contemporary) materials but is absent in fossil fuels, which are much older than the

radiocarbon half-life of 5730 years. Radiocarbon is also a robust "tracer", retaining its identity throughout chemical transformations. Consequently, a ^{14}C measurement performed on a sample of particulate matter provides a means of quantitatively distinguishing between the relative contributions of fossil and contemporary carbon sources [*Cooper et al.*, 1981; *Hildemann et al.*, 1994]. These carbon fractions are often referred to as fossil and biogenic carbon [*Lemire et al*., 2002; *Lewis et al*., 2004]. This analysis requires relatively large samples and is too expensive to be used in routine monitoring networks but has been used to assess the fraction of fossil and biogenic carbon in a number of short-term studies throughout the world [*Szidat et al.*, 2006; *Jordan et al*., 2006; *Endo et al*., 2004].

A variety of radiocarbon studies analyzing the fossil and contemporary content of particulate carbon in the United States have been conducted over the past 25 years. Most of these studies have focused on urban centers. An early study conducted in Portland and Eugene, Oregon, in 1977 and 1978 found that 45–95% of the carbon was contemporary in selected filters when biomass burning was thought to be a significant source of carbon (*Cooper et al.*, 1981). In the Los Angeles basin the typical fraction contemporary was 20–43% in 1982 [*Hildemann et al.,* 1994] and 39% in a 1987 study [*Kaplan and Gordon*, 1994]. Similar results for Los Angles were also found by others [*Currie et al*., 1983; *Berger et al.*, 1986]. In Houston, Texas, the fraction of contemporary carbon was 40% in September 1980 [*Dzubay et al*., 1982] and 48% in August 2000 [*Lemire et al.,* 2002]. Samples collected in Albuquerque, New Mexico, in December 1985 were found to have a fraction contemporary of 40–84%, with 71% on average [*Sheffield et al.,* 1994]. A study in Phoenix, Arizona, and Puget Sound, Washington, estimated the fractions contemporary at ~50% for both a winter and summer season in 2004–2006 [*Bench et al*., 2007]. In Denver, Colorado, the fractions contemporary were 25% on average during the 1996–1997 winter and 47% during the summer [*Klinedinst and Currie*, 1999]. In southeastern U.S. urban centers, the fractions of contemporary particulate carbon were found to be 30% in Birmingham, Alabama, 46% in Atlanta, Georgia, and 60% in Pensacola, Florida, during the winter of 2003–2004 [*Zheng et al*., 2006]. And finally, a study in Nashville, Tennessee, during the summer of 1999 found the fraction contemporary varied from 51% to 73% and was 64% on average [*Lewis et al*., 2004].

Sampling of radiocarbon has also occurred in several rural areas near urban centers. At a heavily forested site near Houston, Texas, the fraction of contemporary carbon was found to vary from 44% to 77% [*Lemire et al*., 2002], near Tampa, Florida, it was ~70% [*Lewis and Stiles,*

2006], and south of Birmingham, Alabama, in Centerville 72% of the particulate carbon was contemporary. As part of a larger study, *Bench et al.* [2007] measured the radio carbon at four rural sites within 100 km of urban centers in New Jersey, Iowa, Arizona, and Washington and found that the fractions contemporary varied from 70% to 95%, with an average of 80%.

Sampling has also been conducted at remote sites. In Yosemite National Park, California, during the summer of 2002, the average fraction contemporary was 86% [*Bench and Herckes,* 2004], and from the *Bench et al.* [2007] study, contemporary carbon at the Grand Canyon National Park in Arizona, Rocky Mountain National Park in Colorado, and Sula, Montana, accounted for over 90% of the TC. At the Great Smoky Mountains National Park in Tennessee, *Bench et al.,* [2007] estimated the average fraction contemporary to be 82% in the summer and 90% in the winter, while *Tanner et al.*, [2004] estimated that 71% of the PM10 carbon was contemporary for samples collected in the spring, summer and fall seasons

These studies report on data collected over the past 25 years at different locations and times of years. In addition, they used different assumptions to derive the fraction of contemporary carbon from the radiocarbon data. Nonetheless, the multiple studies of the radiocarbon in the urban and rural areas of the United States generally provide a consistent set of results. Specifically, in the urban centers contemporary carbon accounts for a large fraction of the TC, though generally less than 50%. In the rural but near urban areas, more than half of the carbon is contemporary, and the particulate carbon concentration in remote areas is primarily composed of contemporary carbon.

The preponderance of contemporary carbon is also support by current emission inventories. In a global emission inventory of primary particulate carbon from fossil and biogenic combustion sources, *Bond et al.* [2004] estimate that in North America combustion of fossil fuel accounts for ~22% of the primary particulate carbon. *Park et al.* [2006] suggest that this emission inventory underestimates anthropogenic carbon emissions by a factor of 2. If true, then fossil fuel would account for ~35% of the primary particulate carbon. These results are qualitatively consistent with the radiocarbon results in that the majority of the primary carbon emissions are from contemporary carbon sources. In addition, on- and off-road mobile emissions accounted for about 90% of the fossil carbon emissions, and the highest mobile source emission densities occur in urban areas [U.S. EPA National Emission Inventory

http://www.epa.gov/ttn/chief/net/index.html]. Therefore, a higher fraction of the fossil primary particulate carbon emissions will occur in urban areas compared to rural areas, which is what was found in the radiocarbon studies.

Corroboration of the radiocarbon data analyses also comes from modeling studies. *Zheng et al.* [2006] found good agreement between fossil carbon fractions estimated by radiocarbon and the chemical mass balance receptor model at several sites in the southeastern United States. A modeling study conducted by *Park et al.* [2003], using 1998 emissions and meteorology but climatological average emissions for wildfire, estimated that 62% of the carbon in the western United States was from natural biogenic sources. However, in the eastern United States only 31% of the carbon was estimated to be from natural sources. These are lower bounds to the contributions of contemporary carbon, since the natural particulate carbon concentrations did not include anthropogenic contributions to contemporary carbon such as residential wood burning [*Park et al.*, 2003].

The corroboration of results across the radiocarbon studies and other modeling studies provides some confidence of the large contributions of contemporary carbon to the carbon aerosol in the United States. However, the data are still only from a relatively few locations. Also, the contribution of natural and anthropogenic sources and SOA to the contemporary and fossil carbon fraction is less well understood.

In this work we further analyze the data collected by *Bench and Herckes* [2004] and *Bench et al.* [2007] to examine two issues. First, the differences between the urban and rural concentrations are examined to assess the contributions of the urban areas to the fossil and contemporary carbon concentrations. Second, the radiocarbon data are integrated with EC and OC data from collocated IMPROVE monitoring sites to develop a relationship between the fossil carbon fraction and the fraction of elemental carbon (EC/TC) during a winter and summer season. This relationship is used to derive characteristic EC/TC ratios for fossil and contemporary carbon. These ratios are then used to estimate the contemporary carbon fraction of the particulate carbon concentrations measured in IMPROVE to develop a national map of the contemporary carbon fraction at mostly rural sites in the conterminous United States. Last, the EC/TC ratios are used to develop a semiquantitative estimate of the contribution of secondary organic carbon (SOC) to the fossil and contemporary concentrations during the summer months.

2. Monitoring Networks, Sampling periods and Data Representativeness

Radiocarbon data from two field campaigns were combined and used for the analyses. The first field campaign used HiVol samplers to collect 6-day integrated $PM_{2.5}$ samples at 11 IMPROVE sites throughout the conterminous United States (see Figure 1 and Table 1). The sites were selected to represent geographically diverse areas and, as shown in Figure 1, included sites in two urban centers, five remote areas, and four rural locations that were within 100 km of an urban center at a similar elevation. At most sites samples were collected for one summertime period from June to August and one wintertime period from December to February in 2004 through 2006. A maximum of 13 samples could be collected at a given site each season. Table 1 lists the sample collection periods for each site. The Lake Sugema, Iowa, monitoring site did not operate during the summer sampling period and the Sula, Montana, monitoring site had equipment problems during the winter sampling period, and only two samples were collected. Consequently, the winter Sula, Montana, data are not discussed. *Bench et al.* [2007] reports on and discusses the contemporary and fossil carbon concentrations from this network except for the data collected at Lake Sugema and Sula.

The second field campaign collected 1 to 3 day integrated $PM_{2.5}$ samples at the IMPROVE monitoring site in Yosemite, California, from 14 July to 3 September 2002 [*Bench and Herckes,* 2004]. The samples were collected and analyzed using identical procedures as used by *Bench et al.* [2007].

Sampling at these diverse sites during winter and summer seasons enabled the characterization of the particulate carbon influenced by different source categories and atmospheric processing. Table 1 reports the median and median absolute deviation from the median (MAD) of the fine particulate TC concentrations and fraction of EC, i.e., the EC/TC ratio, for each of the 12 IMPROVE site with HiVol samplers from 2000 to 2004. The MAD is a robust measure of the spread of the distribution around the data's median and is less influenced by the high carbon concentrations resulting from the impact of biomass burning. Consequently, the MAD results in a narrower distribution compared to the standard deviation. As shown, there was large variability in the typical TC concentrations across the sites, with the summer TC varying by a factor of 3 from 0.8 $\mu g/m^3$ at Grand Canyon to 2.4 $\mu g/m^3$ at Brigantine. During the winter months, the range of TC concentrations increased with 0.23 $\mu g/m^3$ at Grand Canyon to 6.9

μg/m^{3}at Phoenix. There were also differences in the seasonal variability of TC across the sites, with higher wintertime TC at the two urban sites, Phoenix and Puget Sound, and higher summertime TC at all other sites.

Different EC/TC ratios are indications of differing source contributions and/or atmospheric processing of gaseous and particulate carbon compounds. During the summer months the EC/TC ratios varied from 0.09 to 0.16 at the rural sites to 0.13 to 0.2 at the near-urban sites and 0.24 to 0.28 at the two urban sites. The EC/TC ratios increased at all sites during the winter, and the differences between the rural, near-urban, and urban sites decreased.

Table 1 also contains the median and MAD of the IMPROVE TC concentrations at each site during the collection of $PM_{2.5}$ samples for the radiocarbon analysis. As shown, the median TC concentrations are within 1 MAD of the 2000–2004 median concentrations for all sites except during the summer at Yosemite and winter at Mount Rainier, where the TC concentrations were larger than typically found. It is known that the increased concentrations at Yosemite were due to smoke from wildfires in southern Oregon and in the Sierra Nevada mountains impacting Yosemite during most of the sampling period [*McMeeking et al*., 2006]. The EC/TC ratios during the radiocarbon sampling periods were also less than or near 1 MAD from the long-term median. The exceptions are during the winter sampling periods at Lake Sugema and Phoenix, where the EC/TC ratios were higher than typical. Overall, these results indicate the TC concentrations and EC/TC ratios during the radiocarbon studies' sampling periods are similar to and representative of the typical values measured at the monitoring sites.

3. Measurement Methods

Following is a brief description of the sample collection and filter analysis procedures. Detailed descriptions are provided by *Bench and Herckes* [2004] and *Bench et al.* [2007]. $PM_{2.5}$ samples were collected using Thermo Anderson Total Suspended Particulate (TSP) HiVol samplers with SA-230-F impactor plates. Samplers were operated at a volumetric flow of 68 m^3/hour, collecting samples for 6 days from Tuesday to Monday on prefired Gellman QM-A quartz fiber filters. Filter blanks were obtained from each site once a month by placing a quartz fiber filter in the sampler for 10 minutes with the pump off. Sampling at Yosemite differed in that the sampler duration was 1 to 3 days as opposed to 6-days at the other sites.

At Lawrence Livermore National Laboratory (LLNL), 25 cm^2 filter punches were taken from the central region of each quartz filter that was analyzed for TC and radiocarbon. Each punch was sealed under vacuum with CuO oxidizer in a quartz tube and combusted at 900 ºC. CO_2 from the combustion was cryogenically isolated from other combustion products and measured manometrically before conversion to graphite by hydrogen reduction using an iron catalyst. $^{14}C/C$ ratios in the graphite samples were measured by accelerator mass spectrometry (AMS). The data were reported as a fraction of the Modern radiocarbon standard (fraction Modern or F_M) [*Stuiver and Polach,* 1977]. Filter blanks were also analyzed for $^{14}C/C$, which was used to correct the samples for positive organic artifacts [*Bench et al.*, 2007]. The F_M on the filter blanks was always smaller than the F_M on the exposed filters, so the correction always increased the aerosol F_M. The increase was typically less than 6%, but there was a greater than 30% increase for the winter samples at Rocky Mountain and Grand Canyon [*Bench et al.*, 2007].

The fraction of Modern carbon was calculated as $F_m = R_a/R_m$, where R_a is the $^{14}C/C$ ratio of a $PM_{2.5}$ aerosol sample and R_m is the $^{14}C/C$ ratio in modern carbon in 1950. Fossil carbon has $F_m = 0$ and contemporary or biogenic carbon should have $F_m = 1$. However, due to above-ground testing of nuclear bombs in the 1950s and 1960s, the $^{14}C/C$ levels in the atmosphere increased and have been decreasing ever since. For this study, the F_m in the contemporary component was taken to be $F_m = 1.08$ +/- 0.06 Modern. This value corresponds to the average $^{14}C/C$ ratio of contemporary material over the time period 1999–2005, with an uncertainty that corresponds to the difference between the maximum and minimum $^{14}C/C$ ratio over this time period. Therefore, the fraction of contemporary carbon, F_c, in the aerosol samples was estimated by $F_c = F_m/(1.08$ +/- 0.06) and the fraction of fossil carbon, $F_f = 1 - F_c$. A large source of contemporary carbon is from biomass burning. The carbon released by biomass burning may have been sequestered before 1999 and have an F_m larger than 1.08 Modern. For example, the average F_m of wood from 50 year old trees is 1.3 Modern[*Lewis et al.,* 2004]. In such cases, the F_c is will be an overestimate.

Analytical uncertainty in the total carbon mass and F_m measurements were examined using replicate analyses from eight filters [*Bench and Herckes*, 2004], which showed that both carbon mass and F_m were within the reported analytical measurement uncertainties. Collocated samplers were located in Phoenix, Arizona, during the winter sampling period. The observed error in the total carbon from the comparison of the collocated samples was 8%, but only 1.3% for the F_m [*Bench et al.*, 2007]. Bounding calculations were also conducted to test the sensitivity of F_c on the

assumed F_m in the contemporary carbon and the filter blank correction. It was found that the results were robust and relatively insensitive to these factors [*Bench et al.*, 2007]. However, there were samples with F_c significantly greater than 1. This occurred at sites likely to be impacted by biomass burning and could be due to an underestimation of the radiocarbon content of contemporary material.

Following the work by *Bench et al.* [2007], samples from the Tonto, Phoenix, Puget Sound, and Mount Rainier monitoring sites were analyzed for OC and EC by TOR at the Desert Research Institute [*Chow et al*., 1993]. Comparisons of the TC from the manometric and TOR analyses showed excellent precision with $r^2 = 0.94$. However, the TC by TOR was 25% smaller. The difference was found to be due to inhomogeneous deposits on the quartz fiber filters with the highest deposits at the center of the filter, where the filter punches for the AMS analysis were taken, and the lowest deposits in the corners of the filters, where the filter punches for the TOR analysis were taken. The inhomogeneity was not found in the replicate AMS analyses because all punches were taken near the center of the filters. Due to the inhomogeneity, the absolute values are likely biased high by 10–15%; however, this bias does not affect fractional results such as F_c and F_f.

4. Results and Discussion

4.1. Seasonal Fossil and Contemporary Carbon Concentrations

The seasonal concentrations of the fossil and contemporary carbon and the range in the individual samples are summarized in Figure 2. As shown, the summer contemporary carbon concentrations are rather uniform across the sites, ranging from 1.3 to 2.4 $\mu g/m^3$ at most sites. Yosemite was unique, with an average summertime contemporary carbon concentration of 6.8 $\mu g/m^3$, due to smoke from wildfires that impacted the site during most of the sampling period [*McMeeking et al.,* 2006]. There was more variability during the winter, with the average contemporary carbon concentrations ranging from less than 0.5 $\mu g/m^3$ at Rocky Mountain and Grand Canyon to 2.8 $\mu g/m^3$ at Puget Sound and 5.8 $\mu g/m^3$ at Phoenix. During both the winter and summer there was large variability in the individual samples, with the 6-day concentrations varying by a factor of 2 to 10 at a given site. The fossil carbon concentrations at the two urban sites were similar to the contemporary carbon concentrations during both the summer and winter.

The fossil carbon at the other sites was less than the contemporary carbon, with small concentrations at less than 0.5 $\mu g/m^3$ for both seasons.

The seasonal variability in the contemporary and fossil carbon concentrations varied across the sites. At both urban sites the winter contemporary and fossil carbon concentrations were larger than during the summer, with the Phoenix winter concentrations more than a factor of 2 larger. At the near-urban site, Brigantine, the summer and winter concentrations are similar. At all other sites the contemporary carbon concentrations were larger during the summer than winter by a factor of 1.5 at Mount Rainier to a factor of 6 at Rocky Mountain. The concentrations of fossil carbon at the rural western U.S. sites Mount Rainier, Grand Canyon, and Rocky Mountain were also larger during the summer. But there was little to no difference between the summer and winter fossil concentrations at the three eastern U.S. sites and Tonto, Arizona.

Figure 3 presents the average winter and summer fractions of the total carbon that are contemporary and the range in the individual samples at each site. As shown, there is less site to site, sample to sample, and winter to summer variation than seen for the contemporary and fossil carbon concentrations. At the two urban sites the fractions of contemporary carbon are about 50% during both seasons. The fractions contemporary increase to ~80% at the four near-urban sites, Mount Rainier, Tonto, Lake Sugema, and Brigantine, except for the winter season at Mount Rainier and Tonto, which were 97% and 70%, respectively. At the rural sites, Yosemite, Grand Canyon, Sula, Rocky Mountain, Great Smoky Mountains, and Proctor Maple, the fraction contemporary carbon varied from ~82% to 100% with an average of 92%. At all of the rural sites, the winter and summer fractions contemporary were within 10%.

4.2. Urban Excess Fossil and Contemporary Carbon

As shown in Figure 1, the fine particulate total carbon concentrations at most urban monitoring sites are larger than at the neighboring rural sites. This is most pronounced in the western United States where the annual TC concentrations at urban monitors such as Denver, Colorado, Salt Lake City, Utah, and Phoenix, Arizona, are more than a factor of 2 larger than neighboring rural sites. If the concentrations at the rural sites are representative of the regional background concentrations, then the increase in carbon concentrations, or urban excess, is a measure of the influence of the urban area on the particulate carbon concentrations. This increase will be due to primary and secondary particulate carbon from urban sources and possibly due to

enhanced SOA formation rates from the background organic gases due to the higher availability of oxidants in the urban area.

The assessment of the urban excess has two complicating factors. First, airmass transport between the urban and rural sites will occur. Consequently, on average the carbon concentrations at the rural site will have contributions from the urban areas, resulting in an underestimation of the urban excess. On the other hand, the urban and rural areas could have different particulate carbon removal rates. For example, urban areas tend to have higher temperatures than neighboring rural areas, i.e., the urban heat island effect, which could cause volatilization of some of the organic aerosol, causing an underestimation of the contribution from the urban sources.

The radiocarbon monitoring network had two urban/rural pairs of sites in which an urban excess could be examined. In the northwestern United States, the rural Mount Rainier site was located 88 km to the southeast of the urban Puget Sound site, and in the southwestern United States, the rural Tonto site was located 92 km east of the urban Phoenix site (Figure 1). Examination of back trajectories to Tonto and Mount Rainier showed that during both the summer and winter seasons transport frequently occurred between the urban and rural sites, though it occurred more often during the summer months. Therefore, the rural sites are influenced by the urban emissions, and the excess will likely underestimate the impact of the urban area on the concentrations. However, on average the urban influence on the neighboring rural sites should be small, since, as shown in Figure 1 and discussed by *Malm et al.* [2004], the Mount Rainier and Tonto carbon concentrations are similar to more remote receptor sites farther from the urban centers.

The contemporary and fossil carbon concentrations and urban excesses for the Puget Sound and Mount Rainier sites are presented in Figures 4 and 5. Note that due to the inhomogeneity of the sample deposit the concentrations and urban excesses are likely overestimated by 10–15%. As shown in Figure 4, the average summer urban excess at Puget Sound for the contemporary carbon was small, 0.23 $\mu g/m^3$ or 11% of the Puget Sound contemporary carbon concentration, but the fossil carbon excess was 1.56 $\mu g/m^3$, 77% of the Puget Sound's fossil carbon concentration. The summer contemporary carbon concentrations were also similar for the 6-day samples and were correlated at $r = 0.8$ (Figure 5). Although the Puget Sound fossil carbon concentrations were four times higher than at Mount Rainier, their

concentrations were correlated with r = 0.7. During the winter, the average fossil carbon at Mount Rainier was near 0, but ~2.5 $\mu g/m^3$ at Puget Sound. The Puget Sound contemporary carbon concentrations were also more than twice that measured at Mount Rainier. In addition, the fossil and contemporary carbon at Puget Sound and Mount Rainier were not correlated (Figure 5).

The contemporary and fossil concentrations and urban excesses for the Phoenix and Tonto sites are presented in Figures 6 and 7. The Phoenix urban excess has a similar seasonal pattern to Puget Sound. During the summer the average contemporary urban excess is small at 0.42 $\mu g/m^3$ or 17% of the Phoenix contemporary carbon concentration, while the fossil urban excess is 1.53 $\mu g/m^3$ or 81% of the Phoenix fossil carbon concentration. During the winter, both fossil and contemporary carbon have large urban excesses of 5.1 $\mu g/m^3$ and 4.5 $\mu g/m^3$, respectively, which represents more than 80% of the Phoenix winter fossil and contemporary carbon. The Phoenix and Tonto fossil and contemporary carbon during both the summer and winter were not correlated.

These results imply that most of the fossil carbon at Puget Sound and Phoenix was due to local sources during both winter and summer. This is expected, due to increased emissions from fossil-carbon-rich sources, such as mobile sources, relative to the rural sites. Receptor modeling using aerosol concentrations collected in Phoenix from 1995 through 1998 attributed about 50% of the $PM_{2.5}$ to the carbon-rich mobile sources [*Ramadan et al.*, 2000; *Lewis et al.,* 2003]. In Seattle, Washington, mobile sources were estimated to contribute to 30–40% of the $PM_{2.5}$ during the 2000–2001 winter season [*Kim et al.,* 2004].

The small difference and the high correlation in the summertime contemporary carbon between Puget Sound and Mount Rainier indicate that the two monitors were influenced by a similar set of regional sources and the urban area does not appreciably contribute to the contemporary carbon or enhance the formation of contemporary SOA. Two important sources of contemporary carbon are biogenic SOA and biomass burning. The Northwest is a heavily forested area with high emissions of turpenes [*NOAA*, 2007a], precursors to biogenic SOA, so biogenic SOA is a likely contributor. Examination of the satellite-derived fire products from the National Oceanic and Atmospheric Administration's (NOAA) Hazard Mapping System (HSM) [*NOAA,* 2007b] identified few fires near the receptors. However, there were several large fires to the east, and smoke from these fires likely impacted the receptor in late July and the middle of August. The Phoenix contemporary carbon excess was also small during the summer, but 6-day

concentrations were not correlated. The lack of correlation was partly due to wildfires in the vicinity of Phoenix and Tonto during most of the summer sampling period. NOAA's HSM fire product [*NOAA*, 2007b] indicates that the most intense activity was from 29 June 2005 through 27 July 2005 when the highest contemporary carbon concentrations occurred. Biogenic VOC emissions also occur in Arizona, though at a much smaller rate than in the Northwest (http://www.epa.gov/asmdnerl/biogen.html).

During the winter, the contemporary urban excess was more than 50% at both Puget Sound and Phoenix. In addition, the winter contemporary carbon concentrations decreased at the rural sites compared to the summer, but increased at the urban sites. The decrease at the rural sites can partly be attributed to little to no wildfire activity [*NOAA*, 2007b] and reduced biogenic SOA [*Lack et al.*, 2004]. The increased contemporary carbon at the urban sites indicates increased contributions from anthropogenic sources. In Puget Sound, residential wood burning has been identified as a significant contributor to particulate carbon during the winter months; for example, *Kim et al.* [2004] estimate residential wood burning accounted for 45% of the measured $PM_{2.5}$ during the winter of 2000–2001. In Phoenix, receptor modeling estimated biomass burning during the winter months accounted for only ~10% of the $PM_{2.5}$ concentrations [*Ramadan et al.*, 2000; *Lewis et al.,* 2003].

Residential wood burning is not the only anthropogenic source of contemporary carbon. In a study conducted to understand the large fraction of contemporary carbon in Los Angeles, California, *Hildemann et al.* [1994] concluded that the contemporary carbon was largely due to anthropogenic sources from fireplaces, charcoal broilers, paved road dust, and cigarette smoke.

4.3. Relationship of Fossil and Elemental Carbon Concentrations

OC aerosol is a mixture of primary and secondary fossil and contemporary carbon, while, theoretically, EC is a mixture of only primary fossil and contemporary carbon. Carbon concentrations are generally measured using thermal optical methods where the EC and OC split is operationally defined. Therefore, EC concentrations can possibly contain contributions from SOA. Circumstantial evidence for this was seen in a field study conducted in Yosemite, California, during 14 July through 5 September 2002. During this time period the EC/TC ratio was relatively constant [*Malm et al.,* 2005], but using a receptor model *Engling et al.*, [2006]

estimated the average contribution of SOA to OC varied from 21% to 82%, depending on the week.

The EC/TC ratios in emissions are source dependent, with fossil combustion typically having larger ratios than biomass combustion. These differences have been used to help distinguish between the contribution of mobile sources, biomass burning, and SOA to TC [*Turpin and Huntzicker*, 1991; *Lim and Turpin*, 2002; *Malm et al.,* 2004; *Chow and Watson*, 2002]. In several studies it has also been shown that the F_f increases with increasing EC/TC ratios [*Lemire et al.,* 2002; *Lewis et al.,* 2004; *Lewis and Stiles*, 2006]. The data collected in this study provides an opportunity to more fully explore and exploit the relationship between the EC and fossil carbon compositions over a number of different sites and for a winter and summer season.

The EC/TC ratios were estimated from the carbon data collected at the collocated IMPROVE samplers. IMPROVE collects 24-h samples every third day, so the two samples during each 6-day radiocarbon sample period were aggregated together. As shown in Figure 8, during both seasons the F_f increased with increasing EC/TC at similar rates, though the intercept during the winter is higher, EC/TC = 0.2, than the summer, EC/TC = 0.13. There is no discernable geographic difference in the relationship, with the fraction fossil and EC/TC ratios for all sites generally scattered around the ordinary least square (OLS) regression lines. However, the precision is low with r^2 of 0.44 and 0.26 for the summer and winter, respectively.

There are two sources of variability in the EC to fossil carbon ratios in Figure 8. The first source is actually variability in the EC/TC ratios from the different sources of fossil and contemporary carbon as well as due to different atmospheric aging. The second source of variability is due to differences in the $PM_{2.5}$ sample collection by the collocated HiVol and IMPROVE samplers. Most important is the fact that the HiVol measured a 6-day integrated sample and IMPROVE measured a 24-h sample every third day. This second error may be large. Comparisons of TC from the IMPROVE and HiVol data had summer and winter r^2 of 0.5 and 0.84, respectively, with the IMPROVE TC ~20% smaller than the HiVol TC during both seasons. The bias is likely due to the inhomogeneity of the HiVol samples. However, these correlations are lower than the correlation between the TC from the TOR and manometric analysis from the same HiVol filters, which had an $r^2 = 0.94$. This decreased precision is due to the additional uncertainty from the different samplers, operation, and sampling durations.

In order to reduce the uncertainty and inherent variability, the radiocarbon and IMPROVE data were aggregated over each season for each site. The EC/TC ratios were calculated as the ratio of average EC and TC per the recommendation of *Chu et al.* [2005]. As shown in Figure 9, the relationships have improved, with the r^2 increasing to 0.72 for the summer and 0.87 for the winter. The strength in the linear relationship between the fossil/contemporary carbon content and EC/TC ratios is surprising considering that the data are from urban and remote sites in different climatic regions across the United States. However, the variability in the EC/TC ratios does increase at fossil fractions below 0.1 (Figure 9).

The linear relationship implies that the average EC/TC ratios for fossil and contemporary carbon are relatively constant across the sites. Based upon this assumption, characteristic EC/TC ratios for fossil, $(EC/TC)_f$, and contemporary, $(EC/TC)_c$, carbon were derived by using the OLS regression lines to estimate EC/TC ratios at $F_f = 1$ and $F_f = 0$, respectively. As shown in Table 2, the fossil and contemporary carbon EC/TC ratios were seasonal, with higher EC/TC ratios during the winter than summer. Part of the increased winter EC/TC is likely due to a decrease in the SOA contribution to total carbon. In addition, the mix of sources contributing to the carbon during the winter and summer will likely be different. For example, wildfires are a large contributor to carbon aerosol, and wildfire activity is at a minimum during the winter months [*Westerling et al.*, 2006].

Lemire et al. [2002] also examined the relationship between the F_m and EC/TC for 13 samples collected in and near Houston during August 2002, with sampling durations of 6–24 h. They found a strong relationship, with $r^2 = 0.86$. If these data are converted to F_c using a factor of 1.08, then the characteristic EC/TC ratios for fossil and contemporary carbon are 0.38 and -0.14, respectively. The fossil EC/TC ratio is similar to the summer value of 0.36 derived in this study, but the contemporary EC/TC ratio is not. Part of the discrepancy is due to the fact that *Lemire et al.* [2002] used a TOT method to measure OC and EC, while TOR was used in this study, and it is known that the EC by TOR is larger than EC by TOT [*Chow et al.*, 2004]. In addition, the fossil carbon and EC/TC relationship may not be linear over the short sampling times used in the *Lemire et al.* [2002] study, which could cause the negative contemporary EC/TC ratio.

4.3.1. Evaluation of the Fossil and Contemporary Carbon EC/TC Ratios

Fossil and contemporary carbon EC/TC ratios can also be estimated from sources profiles of primary emissions and from ambient samples analyzed for carbon by TOR. The majority of primary fossil carbon aerosol is from mobile sources. *Gillies and Gertler* [2000] summarized over 200 source profiles from light-duty gasoline vehicles (LDGV), diesel vehicles, and a mix of LDGV and diesel vehicles. The profiles were from the Environmental Protection Agency's (EPA) SPECIATE database [*U.S. EPA*, 1999], the Desert Research Instituted (DRI) source profile database [*Gillies and Gertler*, 2000], the Northern Front Range Air Quality Study (NFRAQS) [*Fujita et al.*, 1998; *Watson et al.*, 1998], and source profiles developed by the College of Engineering Center for Environmental Research and Technology (CE-CERT) at the University of California, Riverside [*Norbeck et al.*, 1998]. The source profiles included a wide variety of vehicles under different operating conditions and states of maintenance. As shown in Table 3, there was a broad range of EC/TC for LDGV and diesel, with EC accounting for ~2% to ~90% of the measured carbon. The EC/TC averages ± standard deviations were 0.34 ± 0.22 and 0.61 ± 0.25 for LDGV and diesel, respectively. The DRI database also contained source profiles from 64 mobile-source-dominated ambient samples. The benefit of these source profiles is that they contain contributions from a real-world distribution of vehicles. However, they also likely contain contributions from nonmobile sources. The average EC/TC ratio from these results was 0.4 ± 0.14, which is between the average LDGV and diesel ratios, with a narrower distribution.

Table 4 summarizes the primary EC/TC ratios from the combustion of biogenic material, including mixed vegetation, prescribed fires, agricultural fields, residential wood burning, and meat cooking. The EC/TC ratios were from the EPA's SPECIATE database, source profiles developed for southwestern Texas [*Chow et al*., 2004], and a compilation of biomass burning source profiles of grass/savanna and temperate and tropical forests [*Reid et al*., 2005]. As shown, the variability of the EC/TC ratios in individual source profiles is smaller than for the mobile sources, varying from 0 to 0.46. The average of the composite EC/TC ratios across the studies is 0.12, with a range of 0–0.21.

The fossil and contemporary carbon EC/TC ratios can also be estimated from the range of EC/TC values from the IMPROVE TOR data. Figure 10 presents the scatter plot of EC and TC from all 163 IMPROVE rural sites and 13 urban sites for the winter and summer season during

June 2004 through February 2006. The rural and urban sites were located throughout the United States (Figure 1). During the winter and summer, there are hard edges in the data's scatter. These edges are an indication of contributions from a single source type [*Henry*, 1997]. The 90^{th} and 10^{th} percentiles of the EC/TC ratios were used to estimate the slope of these edges, and the 82^{th} and 98^{th} and 2^{nd} and 18^{th} percentiles were used as a measure of their variability. The results are presented in Table 5.

The urban sites have large contributions from fossil carbon sources, and EC/TC for fossil carbon is larger than for contemporary carbon. Therefore, the upper edges of the urban EC and TC data are interpreted as the characteristic $(EC/TC)_f$. Since SOA will only decrease the EC/TC ratios, the upper edge of the urban scatter plots are also likely to have little contribution from SOA. This assumption is supported by the fact that the 90^{th} percentiles of the urban EC/TC ratios during the winter and summer are similar at 0.44 and 0.41, respectively, and the wintertime organic carbon in urban areas are thought to be primary in origin [*Chu and Macias,* 1981; *Strader et al.*, 1999; *Chu et al.,* 2004]. The $(EC/TC)_c$ is estimated by the lower edge of the scatter at the rural sites, based on the fact that contemporary carbon is the largest contributor to the rural sites and the $(EC/TC)_c$ is smaller than for fossil carbon. However, these are also likely to have contributions from SOA, particularly during the summer months, and should be considered as ratios for contemporary and SOA-dominated carbon concentrations. As shown, the estimated contemporary carbon EC/TC ratio for winter is 0.16 and is 0.07 for summer.

In Figure 11, the fossil and contemporary EC/TC ratios derived from the radiocarbon data are compared to the EC/TC ratios estimated from the measured source profiles and the analysis of EC and TC data. The error bars for the radiocarbon EC/TC ratios are the 95% confidence intervals in Table 2. The measured source profiles for fossil carbon and error bars are from the mixed ambient samples and standard deviations in Table 3, while the average EC/TC and its range in Table 4 are used for the contemporary carbon ratios. As shown, there is good correspondence between the $(EC/TC)_f$ across the three methods for both seasons, with all three methods within 5–15% of each other. This is within the estimated range of EC/TC values for each method. There is more variability in the comparison of the $(EC/TC)_c$. During the winter, the average $(EC/TC)_c$ from the radiocarbon is 20% to 60% greater than the estimate from the TOR data and source profiles, respectively, and in fact is near or above the their upper range. The radiocarbon $(EC/TC)_c$ is also above or at the upper end of the range of $(EC/TC)_c$ estimated from the source

profiles and TOR data. During the summer, the average $(EC/TC)_c$ estimated by the radiocarbon is about equal to the average values from the source profiles and twice the ratio estimated from the TOR data.

The comparison of the fossil and contemporary EC/TC ratios is somewhat confounded by the different contributions of SOA to the total carbon in the three methods. SOA formation is at a minimum during the winter months, so the fossil and contemporary EC/TC ratios from all three methods are mostly primary carbon and should be directly comparable. Therefore, these results indicate that the winter $(EC/TC)_f$ is consistent across the methods, but the winter $(EC/TC)_c$ estimated from the radiocarbon data is higher than the other two methods.

During the summer, the EC/TC ratios from radiocarbon will most likely be influenced by SOA, but the ratios from the measured source profiles are meant to only reflect primary particulate emissions. The EC/TC ratios from the TOR data will also be influenced by SOA. This is thought to be small for the fossil ratios, but likely large for the summer contemporary ratios. As expected, the summer $(EC/TC)_c$ estimated from the TOR data is smaller than the other estimates. The summer radiocarbon $(EC/TC)_f$ ratios are also smaller than the other methods, which is consistent with these data being more influenced by SOA. The summer radiocarbon $(EC/TC)_c$ ratios should also be smaller than the $(EC/TC)_c$ from the source profiles. However, the radiocarbon and source profiles have similar ratios, indicating that the radiocarbon $(EC/TC)_c$ is higher than expected. Consequently, the $(EC/TC)_c$ appear to be high for both the winter and summer seasons.

All three methods are indirect measures of the ambient $(EC/TC)_f$ and $(EC/TC)_c$. Ideally, one would directly measure the fractions fossil and contemporary in the EC and OC fractions of the particulate carbon. *Szidat et al.* [2006] have done this for samples collected in Zurich, Switzerland, during 12 August to 8 September 2002 and 17 February to 26 March 2003. They found a high correlation between fossil OC and fossil EC with $r^2 = 0.8$ and OC/EC = 1.47 ± 0.08 or $(EC/TC)_f = 0.41$. This is between the summer $(EC/TC)_f$ of 0.36 and winter $(EC/TC)_f = 0.46$ found in this study. The correspondence is encouraging; but *Szidat et al.* [2006] used a different thermal technique than TOR for separating the EC and OC fractions. It is not known how the OC/EC split between the two methods differs and what impact this has on the results.

4.4. The Fraction Contemporary Carbon at IMPROVE Monitoring Sites

The OLS regression line in Figure 9 relates EC/TC to the F_f, and can be written as

$$(EC/TC) = \left[(EC/TC)_f - (EC/TC)_c\right] * F_f + (EC/TC)_c \quad (1)$$

where $(EC/TC)_c$ and $(EC/TC)_f$ are the characteristic EC/TC ratios for contemporary and fossil carbon. Solving equation (1) for the F_f, F_c can be written in terms of the EC/TC ratios:

$$F_c = (1 - F_f) = \frac{(EC/TC)_f - (EC/TC)}{(EC/TC)_f - (EC/TC)_c} \quad (2)$$

$F_c = 0$ *if* $EC/TC < (EC/TC)_f$
$F_c = 1$ *if* $EC/TC < (EC/TC)_c$

Equation (2) and the $(EC/TC)_c$ and $(EC/TC)_f$ ratios derived from the radiocarbon data were used to partition the IMPROVE carbon concentrations into fossil and contemporary fractions for the summer (June–August) and winter (December–February) seasons using carbon data from December 2004 through February 2006. Note that the radiocarbon-derived $(EC/TC)_c$ appears to be high compared to other estimates. If the $(EC/TC)_c$ is overestimated, then the calculated F_c will be overestimated and F_f underestimated. The results and their uncertainties are presented in Figure 12. The uncertainties were estimated from the propagation of $(EC/TC)_f$ and $(EC/TC)_c$ standard errors reported in Table 2. The calculation of F_c amplifies the uncertainties in $(EC/TC)_f$ and $(EC/TC)_c$, resulting in errors of 11 to 24 percentage points depending on the season and F_c. The contour intervals used in Figure 12 are 0.15 or approximately 1 standard error.

As shown, F_c was 50% or less of the total carbon at the 13 urban sites for both the winter and summer seasons which is consistent with the radiocarbon measurements in the Phoenix and Puget Sound urban sites. In the rural West, over 90% of the carbon was contemporary during the summer, except in the Southwest where F_c was 80–90% and in southern California where $F_c <$ 60%. In the rural northeastern and southeastern United States, 70–90% of the carbon was contemporary during the summer. However, there is a large region from Illinois to the eastern seaboard where only 50–60% of the carbon was contemporary. This is a region with a high population density and high industrial and farming activities. These F_c values are consistent with those measured at the near-urban sites (Figure 3).

During the winter, the F_c generally decreases in most of the West to 50–80%. However, in much of the northwestern United States, contemporary carbon still composed over 90% of the carbon. In the eastern United States, the winter F_c was 70–90% in the rural areas, which is

generally greater than during the summer. The F_c also increased in the region from Illinois to the eastern seaboard to over 50% percent.

4.4.1. Estimation of the Average SOC Contribution to Fossil and Contemporary Carbon

Turpin and Huntzicker [1991] showed that the OC/EC or EC/TC ratios can be used to estimate the amount of SOA in a sample. The method assumes that all EC is primary, and the average primary EC carbon fraction, $(EC/TC)_P$, from the contributing sources' emissions to the air shed, is relatively constant and known. Under these assumptions, the secondary organic carbon fraction (SOC/TC) can be written as

$$SOC/TC = [1 - (EC/TC)/(EC/TC)_P] \quad (3)$$

where $(EC/TC) \leq (OC/EC)_P$.

This method has been used in a number of studies to estimate the contribution of SOA to total carbon [*Turpin and Huntzicker*, 1991; *Lee and Huang*, 1993; *Castro et al.*, 1999; *Lin and Turpin*, 2002; *Cabada et al.*, 2004; *Yu et al.*, 2004], and *Lemire et al.* [2002], *Lewis et al.* [2004], and *Lewis and Stiles* [2006] used it to qualitatively examine the contributions of SOA to contemporary carbon.

Provided the primary EC carbon fractions for fossil and contemporary carbon are known, equation (3) can be used to estimate the contribution of SOC to fossil and contemporary carbon for known $(EC/TC)_f$ and $(EC/TC)_c$ ratios. Characteristic $(EC/TC)_f$ and $(EC/TC)_c$ ratios were derived for the winter and summer seasons (see Table 2). As discussed, the winter ratios are likely representative of primary particulate carbon emissions, but the summer ratios have contributions from both primary and secondary particulate carbon. Therefore, we have assumed that the winter EC/TC ratios are representative of the primary carbon emission during the summer, and the average fossil and contemporary SOCs were calculated for the characteristic summer EC/TC ratios. As shown in Table 6, the SOC accounted for 41 ± 7.3% of the contemporary OC and 36 ± 15% of the fossil OC. Since fossil carbon has a larger EC fraction, the difference in the SOC contribution increases compared to the TC, with SOC accounting for 36 ± 6.4% of the total contemporary carbon and 23 ± 10% of the total fossil carbon.

These results indicate that a large and similar fraction of both contemporary and fossil OC during the summer months is SOC. However, these are average results based on a limited data set

and limiting assumptions. The primary EC/TC ratios were derived from winter data assuming no SOC. There is likely some SOC during the winter, particularly in the southern sites such as Phoenix, Arizona, and Tonto, Arizona. This will cause an underestimation of the summer SOC. In addition, winter and summer seasons are likely to have different mixtures of fossil and biogenic sources of carbon. For example, wildfires occur more often in the summer than winter. It is not known how this would affect the results. Last, these results do not account for any geographical variation, but emissions of fossil and biogenic SOC precursors and the formation rates of SOC vary widely [*Lack et al.,* 2004]. For example, *Lemire et al*. [2002] showed that a large fraction of the contemporary carbon in and near Houston, Texas, during August was likely SOC, but in a study of the formation of water soluble organic carbon (WSOC) in urban plumes in the northeastern United States, *Sullivan et al.* [2006] found evidence of contributions of fossil sources to secondary WSOC but no direct evidence of the secondary formation of WSOC from biogenic sources.

5. Conclusions

In this study we further analyzed fossil and contemporary carbon concentrations estimated from radiocarbon data collected in two different field studies [*Bench and Herckes*, 2004; *Bench et al.*, 2007]. The combined data were from twelve sites in urban, near-urban, and remote areas and data were collected at most sites during both a winter and summer season. About half of the fine particulate carbon at the urban areas was composed of contemporary carbon. At the near-urban sites, the average fraction of contemporary carbon was 70–97%, depending on the monitoring site location and season, and ~80% on average. The highest fractions of contemporary carbon were at the remote sites, with seasonal averages, F_c, between 82% and 100%. These high levels of contemporary carbon across all sites are consistent with previous radiocarbon monitoring studies as well as current emissions inventories and receptor and source-oriented modeling studies.

Phoenix, Arizona, and Seattle, Washington, each had a monitoring site within the urban area and another rural monitor site within 80 km at similar elevations. These urban/rural pairs were used to examine the urban excess, i.e., a measure of the total contribution from urban sources and possibly enhanced SOA formation rates of the background organic gases. The results indicate that most of the urban fossil carbon during the summer and winter were locally produced. During the summer months, there was a small urban contemporary carbon excess of 11% at Seattle,

indicating that the contemporary carbon concentrations and sources were regionally distributed and the urban area added little to the concentrations. The small urban excess also implies that enhanced formation of biogenic SOA in the urban area is at most a small contributor to the summer urban carbon concentrations. Phoenix also had a small summer contemporary carbon excess, but the interpretation of these results was complicated by varying contributions from local wildfires. During the winter months, the urban contemporary carbon excess was over 50% at Seattle and over 80% at Phoenix. The contemporary carbon was also about half of the measured fine particulate carbon. Consequently, anthropogenic sources of contemporary carbon are likely a significant contributor to the winter carbon concentrations in these two urban centers.

Estimates of EC and OC from TOR analysis were also available at each site. It was found that when the data were aggregated over each season, the fractions of fossil carbon were proportional to the EC/TC ratios across the sites. These results were used to derive characteristic EC/TC ratios for fossil and contemporary carbon. The winter and summer EC/TC ratios for fossil carbon were 0.36 and 0.45, respectively, and for contemporary carbon were 0.12 and 0.19, respectively. The fossil EC/TC ratios are consistent with estimates from measured source profiles and empirically derived EC/TC ratios from rural and urban carbon measurements. However, the contemporary carbon EC/TC ratios were higher compared to the other estimates. A semiquantitative estimate of the average contribution to the summer fossil and contemporary carbon concentrations was made by assuming that the winter EC/TC ratios were representative of primary emissions and the decreased summer ratios were due to increased TC from the formation of SOC. The results indicate that the SOC accounted for more than a third of the fossil and contemporary carbon.

These characteristic fossil and contemporary EC/TC ratios were also used to estimate the average fossil and contemporary carbon concentrations from the IMPROVE fine particulate carbon concentrations to develop a national picture of the contemporary and fossil carbon concentrations at mostly rural locations in the conterminous United States. These results are consistent with the radiocarbon results for the urban, near-urban, and rural sites. One interesting difference is that the fractions of contemporary carbon derived for the IMPROVE sites show more seasonality than from the radiocarbon data. In the western United States, the fractions of contemporary carbon decreased at most sites in the winter relative to the summer, while in the

eastern United States the fractions of contemporary carbon increased at most sites during the winter relative to the summer.

The estimations of the F_c at the IMPROVE monitoring sites and the fossil and contemporary SOC are based on a number of assumptions, most importantly, valid and stable estimates of the fossil and contemporary EC/TC ratios. The derived ratios from the radiocarbon data are consistent with the two other methods used to estimate these ratios. However, as discussed, this comparison was confounded by different contributions of SOC to the carbon concentrations used in the three analyses. A recommendation for future work is to directly measure the fossil and contemporary carbon in the EC and OC fractions of the sampled particulate carbon. To be consistent with this work the method for separating the EC and OC carbon for analysis would need to be equivalent to the IMPROVE TOR carbon analysis technique.

This work was performed under the auspices of the U.S. Department of Energy by University of California, Lawrence Livermore National Laboratory under Contract W-7405-Eng-48.

6. References

Adams, K. M., L. I. Davis Jr., S. M. Japar, D. R. Finley, and R. A. Cary (1990), Measurement of atmospheric elemental carbon: Real-time data for Los Angeles during summer 1987, *Atmos. Environ., 24A*, 597–604.

Bench, G., and P. Herckes (2004), Measurement of contemporary and fossil carbon contents of PM2.5 aerosols: Results from Turtleback Dome, Yosemite National Park, *Environ. Sci. Technol., 38*, 2424–2427.

Bench, G., S. Fallon, B. A. Schichtel, W. C. Malm, C. McDade (2007), Relative contributions of fossil and contemporary carbon sources to PM2.5 aerosols at nine IMPROVE network sites, *J. Geophys. Res.,* accepted for publication.

Berger, R., D. McJunkin, and R. Johnson (1986), Radiocarbon concentration of California aerosols, *Radiocarbon, 28*(2A), 661–667.

Bond, T. C., D. G. Streets, K. F. Yarber, S. M. Nelson, J.-H. Woo, and Z. Klimont (2004), A technology-based global inventory of black and organic carbon emissions from combustion, *J. Geophys. Res., 109*, D14203, doi:10.1029/2003JD003697.

Brewer P. F., and J. P. Adlhoch (2005), Trends in speciated fine particulate matter and visibility across monitoring networks in the southeastern United States, *J. Air Waste Manage. Assoc., 55*(11), 1663–1674.

Birch, M. E., and R. A. Cary (1996), Elemental carbon-based method for monitoring occupational exposures to particulate diesel exhaust, *Aerosol Sci. Technol., 25*, 221–241.

Cabada, J. C., S. N. Pandis, R. Subramanian, A. L. Robinson, A. Polidori, and B. Turpin (2004), Estimating the secondary organic aerosol contribution to PM2.5 using the EC tracer method, *Aerosol Sci. Technol., 38*(S1), 140–155.

Castro, L. M., C. A. Pio, R. M. Harrison, and D. J. T. Smith (1999), Carbonaceous aerosol in urban and rural European atmospheres: Estimation of secondary organic carbon concentrations, *Atmos. Environ., 33*, 2771–2781.

Chow, J. C., and J. G. Watson (2002), Review of PM2.5 and PM10 apportionment for fossil fuel combustion and other sources by the chemical mass balance receptor model, *Energy Fuels*, *16*, 222–260.

Chow, J. C., J. G. Watson, L. C. Pritchett, W. R. Pierson, C. A. Frazier, and R. G. Purcell (1993), The DRI thermal/optical reflectance carbon analysis system: Description, evaluation and applications in U.S. air quality studies, *Atmos. Environ., 27A*, 1185–1201.

Chow, J. C., J. G. Watson, D. Crow, D. H. Lowenthal, and T. Merrifield (2001), Comparison of IMPROVE and NIOSH carbon measurements, *Aerosol Sci. Technol., 34*, 23–34.

Chow, J. C., J. G. Watson, H. Kuhns, V. Etyemezian, D. H. Lowenthal, D. Crow, S. D. Kohl, J. P. Engelbrecht, and M. C. Green (2004), Source profiles for industrial, mobile, and area sources in the Big Bend Regional Aerosol Visibility and Observational study, *Chemosphere, 54*, 185–208.

Chu, S. H. (2005), Stable estimate of primary OC/EC ratios in the EC tracer method, *Atmos. Environ., 39*, 1383–1392.

Chu, S. H., J. W. Paisie, and B. W. L. Jang (2004), PM data analysis—a comparison of two urban areas: Fresno and Atlanta, *Atmos. Environ., 38*, 3155–3164.

Cooper, J. A., L. A. Currie, and G. A. Klouda (1981), Assessment of contemporary carbon combustion source contributions to urban air particulate levels using C-14 measurements, *Environ. Sci. Technol., 15*(9), 1045–1050.

Currie, L. A., G. A. Klouda, R. E. Continetti, I. R. Kaplan, W. W. Wong, T. G. Dzubay, and R. K. Stevens (1983), On the origin of carbonaceous particles in American cities: Results of radiocarbon ‘‘dating’’ and chemical characterization, *Radiocarbon, 25*(2), 603– 614.

Currie, L. A., B. A. Benner, J. D. Kessler, D. B. Lindens, G. A. Klouda, J. V. Marolf, J. F. Slater, S. A. Wise, H. Cachier, R. Cary, J. C. Chow, J. Watson, E. R. M. Druffel, C. A. Masiello, T. I. Eglinton, A. Pearson, C. M. Reddy, O. Gustafsson, J. G. Quinn, P. C. Hartmann, J. I. Hedges, K. M. Prentice, T. W. Kirchstetter, T. Novakov, H. Puxbaum, and H. Schmid (2002), A critical evaluation of interlaboratory data on total, elemental, and isotopic carbon in the carbonaceous particle reference material, NIST SRM 1649a, *J. Res. Natl. Inst. Stand. Technol., 107*, 279–298.

DeBell, L. J., K. A. Gebhart, J. L. Hand, W. C. Malm, M. L. Pitchford, B. A. Schichtel, and W. H. White (2006), Spatial and seasonal patterns and temporal variability of haze and its constituents in the United States, IMPROVE Report IV, *ISSN 0737-5352-74*, 288 pp., Cooperative Institute for Research in the Atmosphere, Colorado State University, Fort Collins, CO 80523.

Dzubay, T. G., R. K. Stevens, C. W. Lewis, D. H. Hern, W. J. Courtney, J. W. Tesch ,and M. A. Mason (1982), Visibility and aerosol composition in Houston, Texas, *Environ. Sci. Technol*., *16*, 514–525.

Engling, G., P. Herckes, S. M. Kreidenweis, W. C. Malm, and J. L. Collett Jr. (2006), Composition of the fine organic aerosol in Yosemite National Park during the 2002 Yosemite Aerosol Characterization Study, *Atmos. Environ., 40*, 2959–2972.

Eatough, D. J., B. Sedar, L. Lewis, L. D. Hansen, E. A. Lewis, and R. J. Farber (1989), Determination of semivolatile organic compounds in particles in the Grand Canyon area, *Aerosol Sci. Technol., 10*, 438–449.

Endo, M., N. Yamamoto, J. Yoshinaga, Y. Yanagisawa, O. Endo, S. Goto, M. Yoneda, Y. Shibata, and M. Morita (2004), C-14 measurement for size-fractionated airborne particulate matters, *Atmos. Environ., 38*(36), 6263–6267.

Flanagan J. B., R. K. M. Jayanty, E. E. Rickman, and M. R. Peterson (2006), PM2.5 speciation trends network: Evaluation of whole-system uncertainties using data from sites with collocated samplers, *J. Air Waste Manage. Assoc., 56*(4), 492–499.

Fujita, E., J. G. Watson, J. C. Chow, N. F. Robinson, L. W. Richards, and N. Kumar (1998), Northern Front Range Air Quality Study, Volume C: Source apportionment and simulation methods and evaluation, prepared for the Cooperative Institute for Research in the Atmosphere, Colorado State University, by Desert Research Institute, Reno, NV.

Gillies, J. A., and A. W. Gertler (2000), Comparison and evaluation of chemically speciated mobile source PM2.5 particulate matter profiles, *J. Air Waste Manage. Assoc., 50*, 1459–1480.

Henry, R. C. (1997), History and fundamentals of multivariate air quality receptor models, *Chemom. Intell. Lab. Syst., 37*, 37–42.

Hegg, D. A., J. Livingston, P. V. Hobbs, T. Novakov, and P. Russell (1997), Chemical apportionment of aerosol column optical depth off the mid-Atlantic coast of the United States, *J. Geophys. Res., 102*, 25,293–25,303.

Hering, S. V., B. R. Appel, W. Cheng, F. Salaymeh, S. H. Cadle, P. A. Mulawa, T. A. Cahill, R. A. Eldred, M. Surovik, D. Fitz, J. E. Howes, K. T. Knapp, L. Stockburger, B. J. Turpin, J. J. Huntzicker, X-Q Zhang, and P. H. McMurry (1990), Comparison of sampling methods for carbonaceous aerosols in ambient air, *Aerosol Sci. Technol., 12*, 200–213.

Hildemann, L. M., D. B. Klinedinst, G. A. Klouda, L. A. Currie, and G. R. Cass (1994), Sources of urban contemporary carbon aerosol, *Environ. Sci. Technol., 28*, 1565–1576.

Husain, L., P. P. Parekh, V. A. Dutkiewicz, A. R. Khan, K. Yang, and K. Swami (2004), Long-term trends in atmospheric concentrations of sulfate, total sulfur, and trace elements in the northeastern United States, *J. Geophys. Res., 109*(D18), Art. No. D18305.

Jacobson, M. Z. (2001a), Global direct radiative forcing due to multicomponent anthropogenic and natural aerosols, *J. Geophys. Res., 106*(D2), 1551–1568.

Jacobson, M. Z. (2001b), Strong radiative heating due to the mixing state of black carbon in atmospheric aerosols, *Nature, 409*(6821), 695–697.

Jordan, T. B., A. J. Seen, G. E. Jacobsen, and J. L. Gras (2006), Radiocarbon determination of wood smoke contribution to air particulate matter in Launceston, Tasmania, *Atmos. Environ., 40*(14), 2575–2582.

Kaplan, I. R., and R. J. Gordon (1994), Non-fossil-fuel fine-particulate organic carbon aerosols in Southern California determined during the Los Angeles aerosol characterization and source apportionment study, *Aerosol Sci. Technol., 21*, 343–359.

Klinedinst, D. B., and L. A. Currie (1999), Direct quantification of PM2.5 fossil and biomass carbon within the Northern Front Range Air Quality Study's domain, *Environ. Sci. Technol., 33*(23), 4146–4154.

Kim, E., P. K. Hopke, T. V. Larson, N. N. Maykut, and J. Lewtas (2004), Factor analysis of Seattle fine particles, *Aerosol Sci. Technol*., *38*, 724–738.

Lack, D. A., X. X. Tie, N. D. Bofinger, A. N. Wiegand, and S. Madronich (2004), Seasonal variability of secondary organic aerosol: A global modeling study, *J. Geophys. Res., 109,* D03203, doi:10.1029/2003JD003418.

Lee, W. G., and R. Huang (1993), Diurnal variation of organic aerosols in a severely polluted atmosphere, *J. Environ. Sci. Health., Part A, 28,* 1565–1579.

Lemire, K. R., D. T. Allen, G. A. Klouda, and C. W. Lewis (2002), Fine particulate matter source attribution for southeast Texas using 14C/13C ratios, *J. Geophys. Res., 107(*D22), 4613, doi:10.1029/2002JD002339.

Lewis, C. W., and D. C. Stiles (2006), Radiocarbon content of PM2.5 ambient aerosol in Tampa, FL, *Aerosol Sci. Technol., 40,* 189–196.

Lewis, C. W., R. E. Baumgardner, R. K. Stevens, L. D. Claxton, and J. Lewtas (1988), Contribution of woodsmoke and motor-vehicle emissions to ambient aerosol mutagenicity, *Environ. Sci. Technol., 22*, 968–971.

Lewis, C. W., G. A. Norris, T. L. Conner, and R. C. Henry (2003), Source apportionment of Phoenix PM2.5 aerosol with the Unmix receptor model. *J. Air Waste Manage. Assoc., 53*, 325–338.

Lewis, C. W., G. A. Kloudab, and W. D. Ellenson (2004), Radiocarbon measurement of the biogenic contribution to summertime PM2.5 ambient aerosol in Nashville, TN, *Atmos. Environ., 38*, 6053–6061.

Lim, H. J., and B. J. Turpin (2002), Origins of primary and secondary organic aerosol in Atlanta: Results of time-resolved measurements during the Atlanta supersite experiment, *Environ. Sci. Technol., 36*(21), 4489–4496.

Malm, W. C., J. F. Sisler, D. Huffman, R. A. Eldred, and T. A. Cahill (1994), Spatial and seasonal trends in particle concentration and optical extinction in the United States, *J. Geophys. Res.*, *99*(D1), 1347–1370.

Malm W. C., B. A. Schichtel, R. B. Ames, and K. A. Gebhart (2002), A 10-year spatial and temporal trend of sulfate across the United States, *J. Geophys. Res.*, *107*(D22), Art. No. 4627.

Malm W. C, B. A. Schichtel, M. L. Pitchford, L. L. Ashbaugh, and R. A. Eldred (2004), Spatial and monthly trends in speciated fine particle concentration in the United States, *J. Geophys. Res.*, *109*(D3), Art. No. D03306.

Malm, W. C., D. E. Day, C. Carrico, S. M. Kreidenweis, J. L. Collett Jr., G. McMeeking, T. Lee, J. Carrillo, B. A. Schichtel (2005), Intercomparison and closure calculations using measurements of aerosol species and optical properties during the Yosemite Aerosol Characterization Study, *J. Geophys. Res.*, *110*, D14302, doi:10.1029/2004JD005494.

McMeeking, G. R., S. M. Kreidenweis, M. Lunden, J. Carrillo, C. M. Carrico, T. Lee, P. Herckes, G. Engling, D. E. Day, J. Hand, N. Brown, W. C. Malm, and J. L. Collett Jr. (2006), Smoke-impacted regional haze in California during the summer of 2002, *Agr. Forest. Meteorol., 137,* 25–42.

NOAA (2007a), Emission Inventory Mapviewer, http://map.ngdc.noaa.gov/website/al/nei99_v3/viewer.htm, accessed January 2007.

NOAA (2007b), Satellite Fire Detections, http://www.ssd.noaa.gov/PS/FIRE/hms.html, accessed January 2007.

Norbeck, J. M., T. D. Durbin, and T. J. Truex (1998), Measurement of primary particulate matter emissions from light-duty motor vehicles, prepared for Coordinating Research Council, Inc., and South Coast Air Quality Management District by the Center for Environmental Research and Technology, College of Engineering, University of California: Riverside, CA.

Park, R. J., D. J. Jacob, M. Chin, and R. V. Martin (2003), Sources of carbonaceous aerosols over the United States and implications for natural visibility, *J. Geophys. Res., 108*(D12), 4355, doi:10.1029/ 2002JD003190.

Park, R. J., D. J. Jacob, N. Kumar, and R. M. Yantosca (2006), Regional visibility statistics in the United States: Natural and transboundary pollution influences, and implications for the regional haze rule, *Atmos. Environ., 40*, 5405–5423.

Ramadan, Z., X. H. Song, and P. K. Hopke (2000), Identification of sources of Phoenix aerosol by positive matrix factorization, *J. Air Waste Manage. Assoc., 50*, 1308–1320.

Reid, J. S., R. Koppmann, T. F. Eck, and D. P. Eleuterio (2005), A review of biomass burning emissions part II: Intensive physical properties of biomass burning particles, *Atmos. Chem. Phys., 5*, 799–825.

Rogge, W. F., M. A. Mazurek, L. M. Hildemann, and G. R. Cass (1993), Quantification of urban organic aerosols at a molecular level: Identification, abundance and seasonal variation, *Atmos. Environ., 27A*, 1309–1330.

Schauer, J. J., W. F. Rogge, L. M. Hildemann, M. A. Mazurek, and G.R. Cass (1996), Source apportionment of airborne particulate matter using organic compounds as tracers, *Atmos. Environ., 30*, 3837–3855.

Sheffield A. E., G. E. Gordon, L. A. Currie, and G. E. Riederer (1994), Organic, elemental, and isotopic tracers of air-pollution sources in Albuquerque, NM, *Atmos. Environ., 28*(8), 1371–1384.

Salvi, S., A. Blomberg, B. Rudell, F. Kelly, T. Sandstrom, S. T. Holgate, and A. Frew (1999), Acute inflammatory responses in the airways and peripheral blood after short-term exposure to diesel exhaust in healthy human volunteers, *Am. J. Repir. Crit. Care Med., 159*, 702–709.

Stuiver, M., and H. A. Polach (1977), Reporting of ^{14}C data, *Radiocarbon*, *19*, 355–363.

Szidat, S., T. M. Jenk, H.-A. Synal, M. Kalberer, L. Wacker, I. Hajdas, A. Kasper-Giebl, and U. Baltensperger (2006), Contributions of fossil fuel, biomass-burning, and biogenic emissions to carbonaceous aerosols in Zurich as traced by 14C, *J. Geophys. Res., 111*, D07206, doi:10.1029/2005JD006590.

Sullivan, A. P., R. E. Peltier, C. A. Brock, J. A. de Gouw, J. S. Holloway, C. Warneke, A. G. Wollny, and R. J. Weber (2006), Airborne measurements of carbonaceous aerosol soluble in water over northeastern United States: Method development and an investigation into water-soluble organic carbon sources, *J. Geophys. Res., 111*, D23S46, doi:10.1029/2006JD007072.

Tanner, R. L., W. J. Parkhurst, and A. P. McNichol (2004), Fossil sources of ambient aerosol carbon based on 14C measurements, *Aerosol Sci. Technol., 38*(S1), 133–139.

Turpin, B. J., and J. J. Huntzicker (1991), Secondary formation of organic aerosol in the Los Angeles Basin: A descriptive analysis of organic and elemental carbon concentrations, *Atmos. Environ., 25A*, 207–215.

Turpin, B. J., J. J. Huntzicker, S. M. Larson, and G. R. Cass (1991), Los Angeles summer midday particulate carbon: Primary and secondary aerosol, *Environ. Sci. Technol., 25*, 1788–1793.

U.S. EPA (1999), SPECIATE: EPA's repository of total organic compound and particulate matter speciated profiles for a variety of sources for use in source apportionment studies, U.S. Environmental Protection Agency, Office of Air Quality Planning and Standards, Research Triangle Park, NC, available from <http://www.epa.gov/ttn/chief/software/speciate/>.

Watson, J. G., E. M. Fujita, J. C. Chow, B. Zielinska, L. W. Richards, W. Neff, and D. Dietrich (1998), Northern Front Range Air Quality Study Final Report, prepared for the Cooperative Institute for Research in the Atmosphere, Colorado State University, by Desert Research Institute: Reno, NV.

Westerling, A. L., H. G. Hidalgo, D. R. Cayan, and T. W. Swetnam (2006), Warming and earlier spring increase western U.S. forest wildfire activity, *Science*, *313*(5789), 940–943.

Yuan, H., K. A. Rahn, and G. Zhuang (2004), Graphical techniques for interpreting the composition of individual aerosol particles, *Atmos. Environ., 38*, 6845–6854.

Yu, S. C., R. L. Dennis, P. V. Bhave, and B. K. Eder, B.K. (2004), Primary and secondary organic aerosols over the United States: Estimates on the basis of observed organic carbon (OC) and elemental carbon (EC), and air quality modeled primary OC/EC ratios, *Atmos. Environ.*, *38,* 5257-5268.

Zheng, M., G. R. Cass, J. J. Schauer, and E. S. Edgerton (2002), Source apportionment of PM2.5 in the Southeastern United States using solvent- extractable organic compounds as tracers, *Environ. Sci. Technol., 36*, 2361–2371.

Zheng, M., L. Ke, E. S. Edgerton, J. J. Schauer, M. Dong, and A. G. Russell (2006), Spatial distribution of carbonaceous aerosol in the southeastern United States using molecular markers and carbon isotope data, *J. Geophys. Res.*, *111*, D10S06, doi:10.1029/2005JD006777.

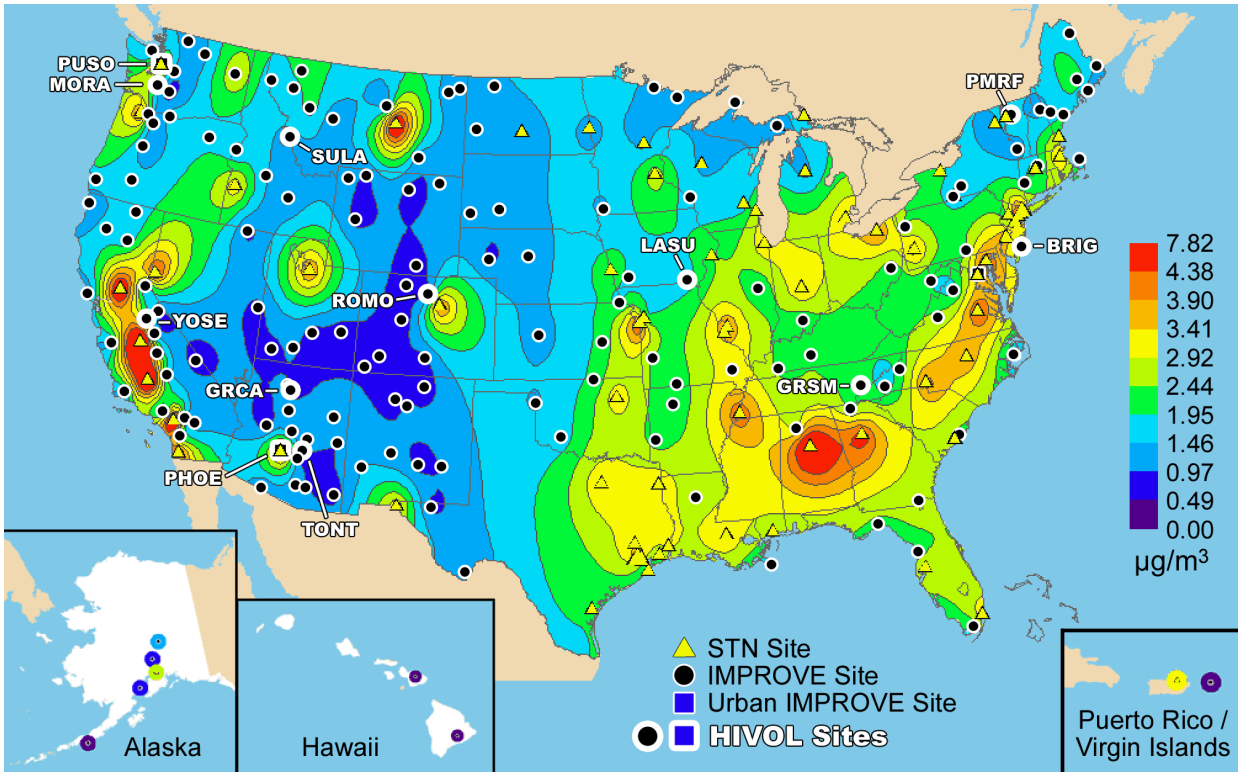

Figure 1. The annual average total particulate carbon at rural and urban locations. The data are from the IMPROVE and EPA Speciated Trends Network averaged over the years 2000–2004 [*DeBell et al.*, 2006]. IMPROVE sites with collocated HiVOL samplers used in the radiocarbon field study are identified on the map. The data are spatially interpolated using a Kriging algorithm to help visualize spatial patterns in the data.

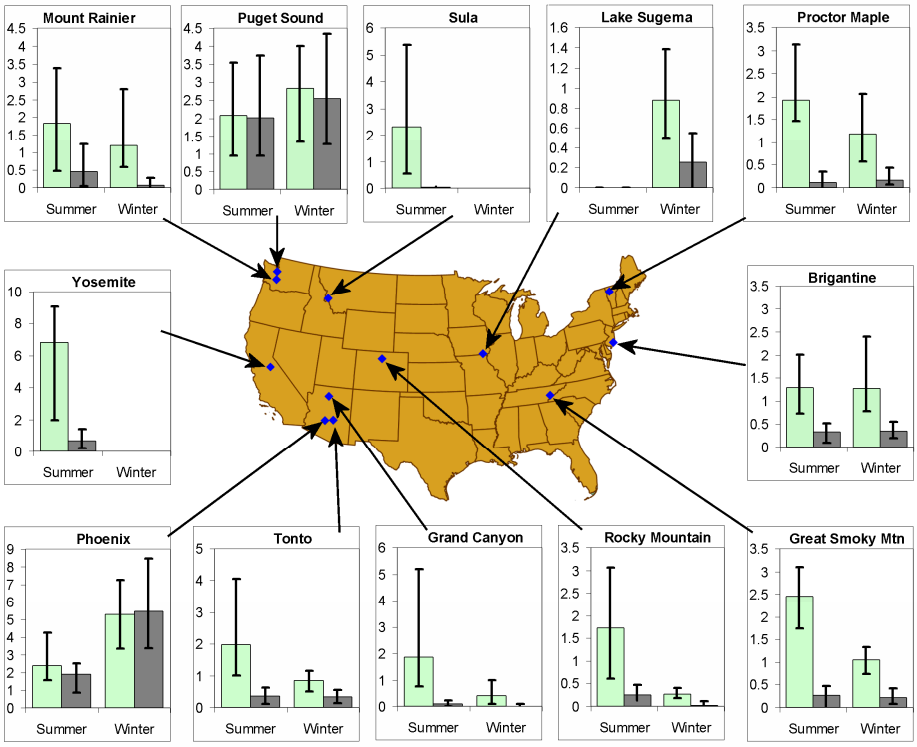

Figure 2. Average seasonal concentrations of contemporary (green bars) and fossil (gray bars) carbon at each monitoring site. The error bars represent the range in the 6-day concentrations in each season.

Figure 3. Seasonal average fraction contemporary carbon at each monitoring site. The error bars represent the range in the 6-day fraction contemporary values in each season. The fraction contemporary is the ratio of average contemporary carbon to average total carbon.

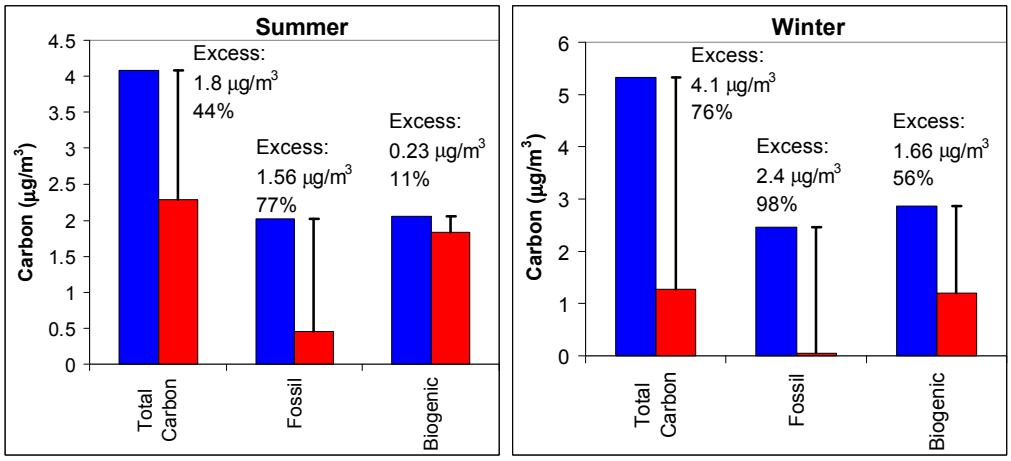

Figure 4. Comparison of the carbon concentrations between the urban Puget Sound (blue bars) and neighboring rural Mount Rainier (red bars) monitoring sites.

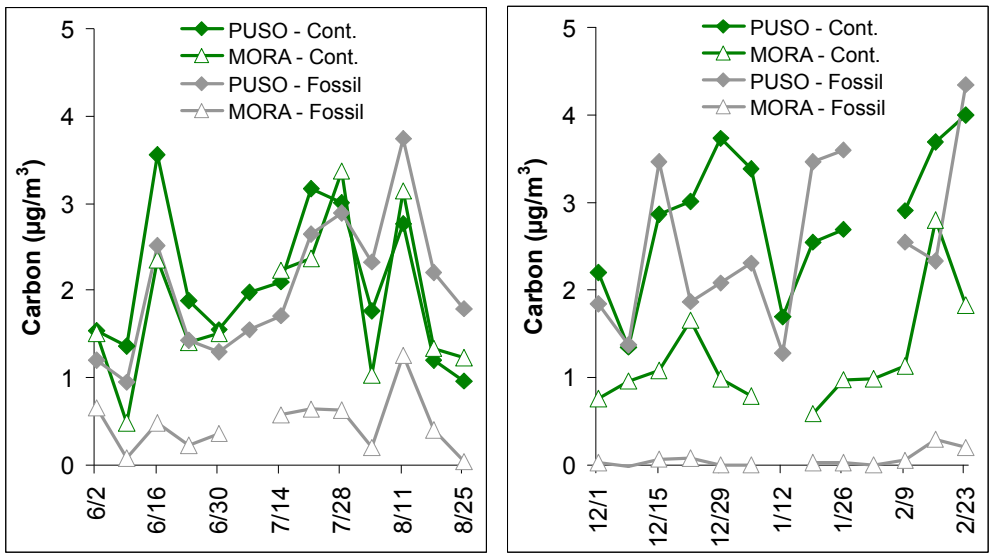

Figure 5. The fossil and contemporary carbon concentrations at Puget Sound (PUSO) and Mount Rainier (MORA) for the summer and winter seasons.

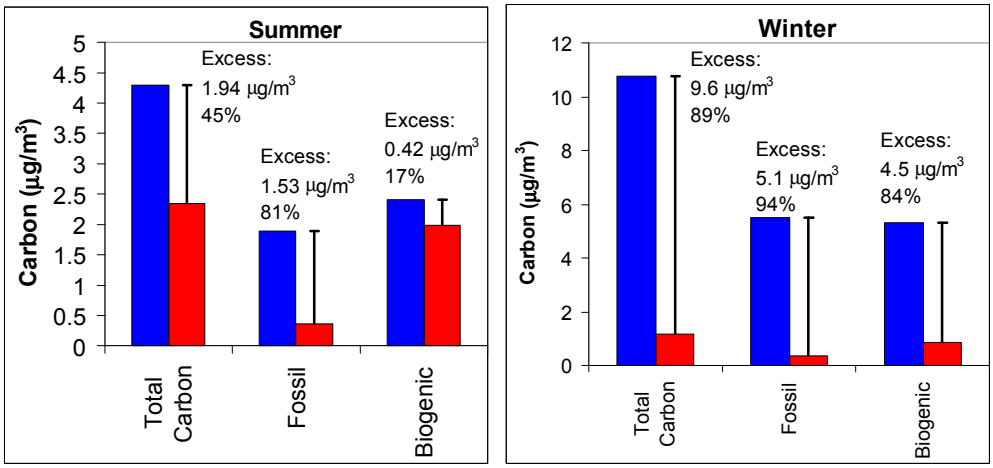

Figure 6. Comparison of the carbon concentrations between the urban Phoenix (blue bars) and neighboring rural Tonto (red bars) monitoring sites.

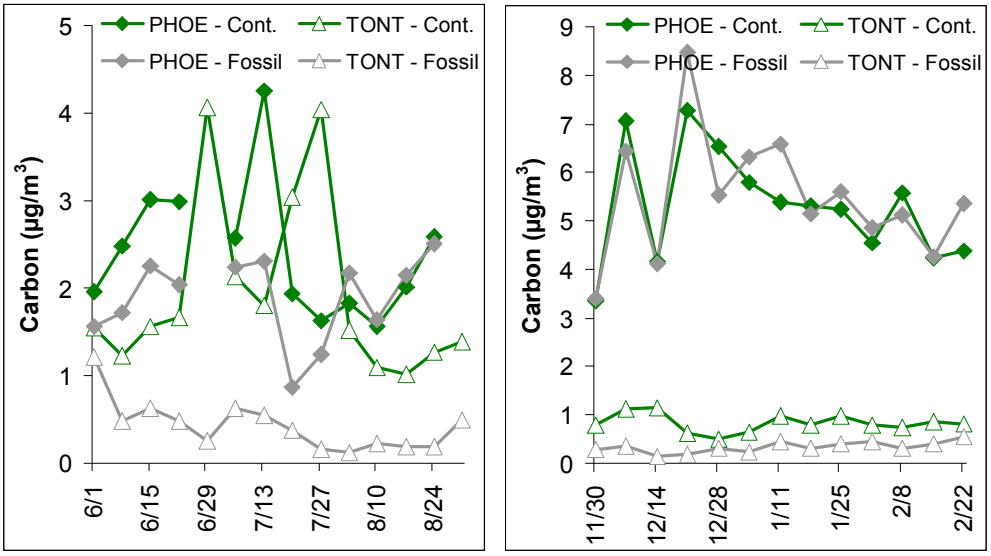

Figure 7. The fossil and contemporary carbon concentrations at Phoenix (PHOE) and Tonto (TONT) for the summer and winter seasons.

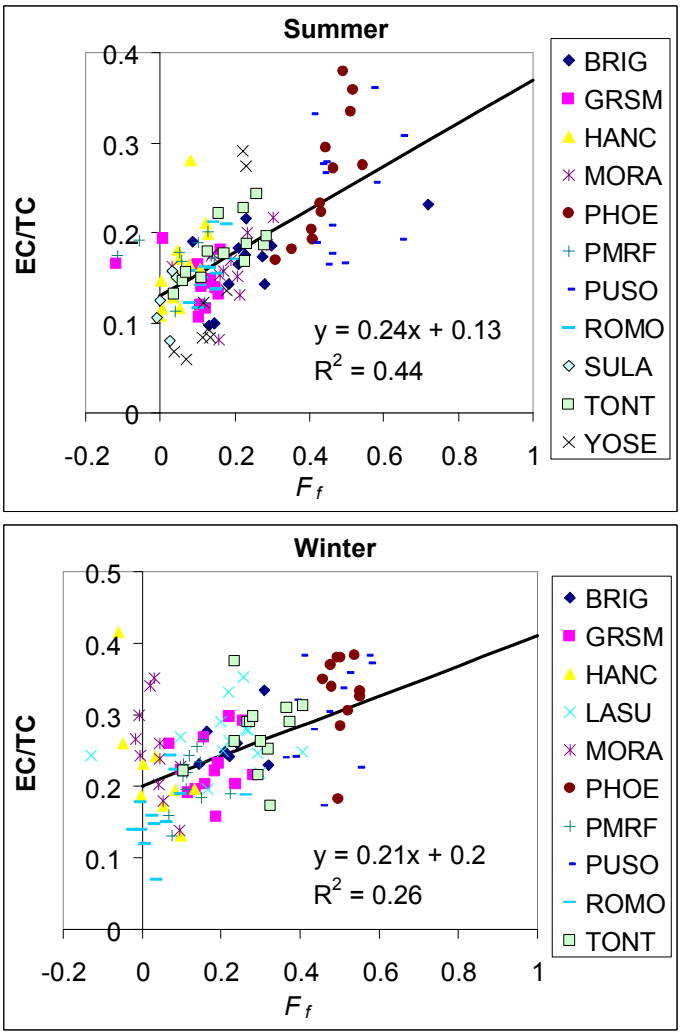

Figure 8. Scatter plot of the F_f and EC/TC ratios for the 6-day sample periods.

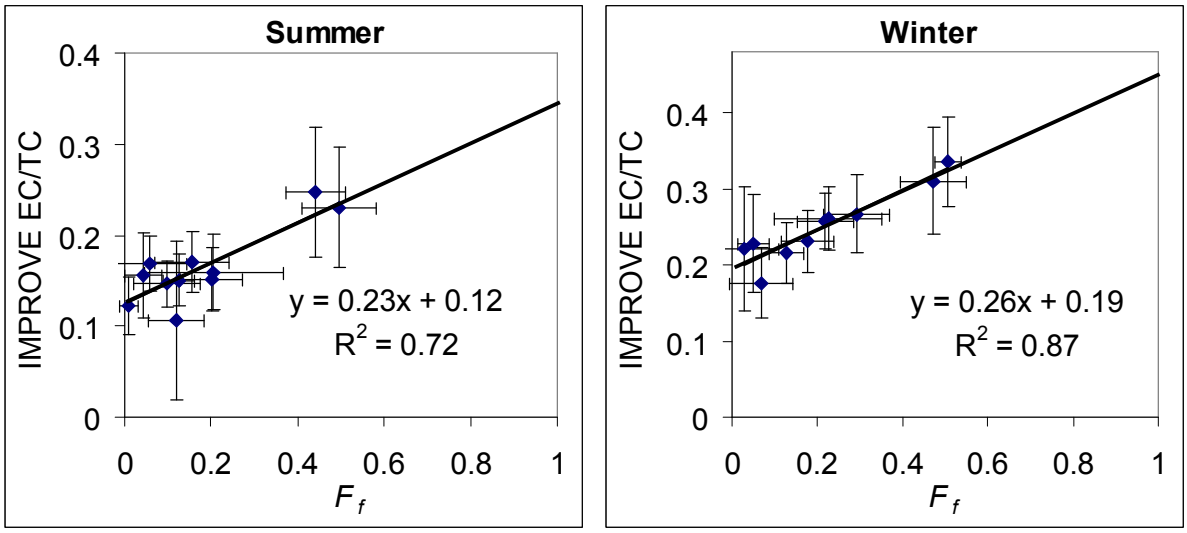

Figure 9. Scatter plot of the F_f and EC/TC ratios for each site averaged over the summer and winter seasons. The error bars the standard deviation of the weekly data values.

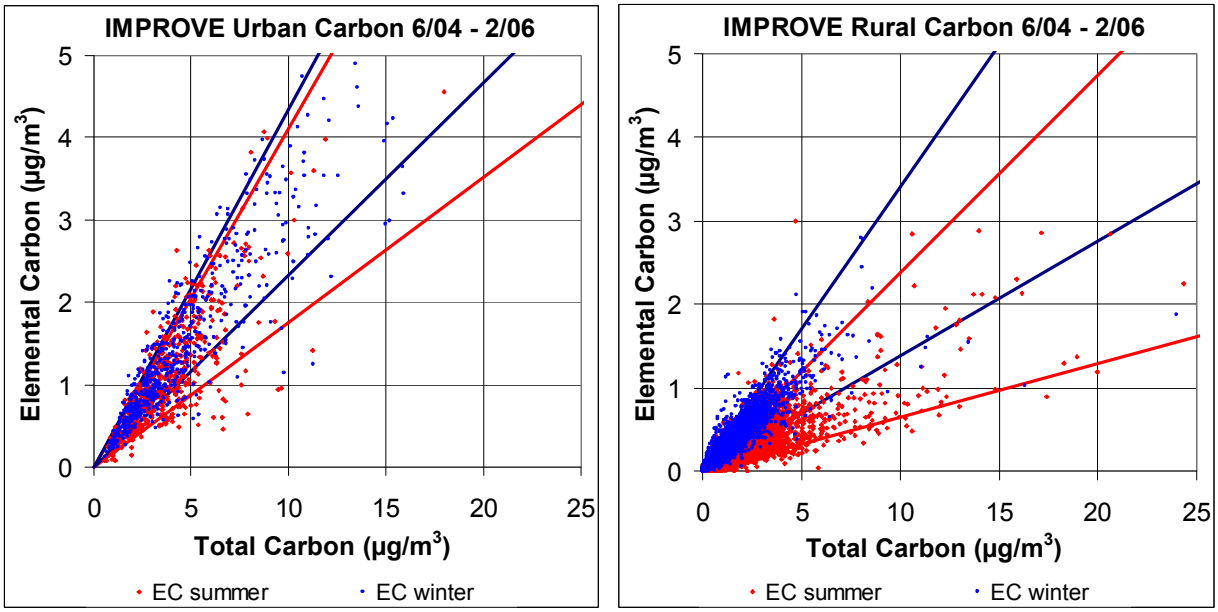

Figure 10. Scatter of the total carbon and elemental carbon concentrations measured at the urban and rural IMPROVE monitoring sites.

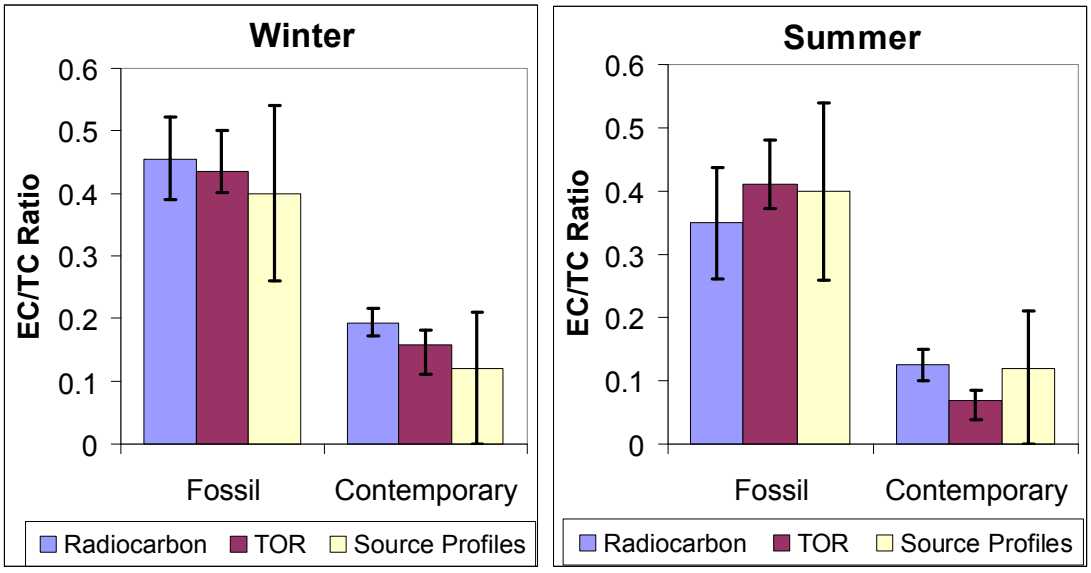

Figure 11. Characteristic fossil and contemporary EC/TC ratios derived from the radiocarbon compared to the EC/TC ratios estimated from source profiles and measured EC and TC data.

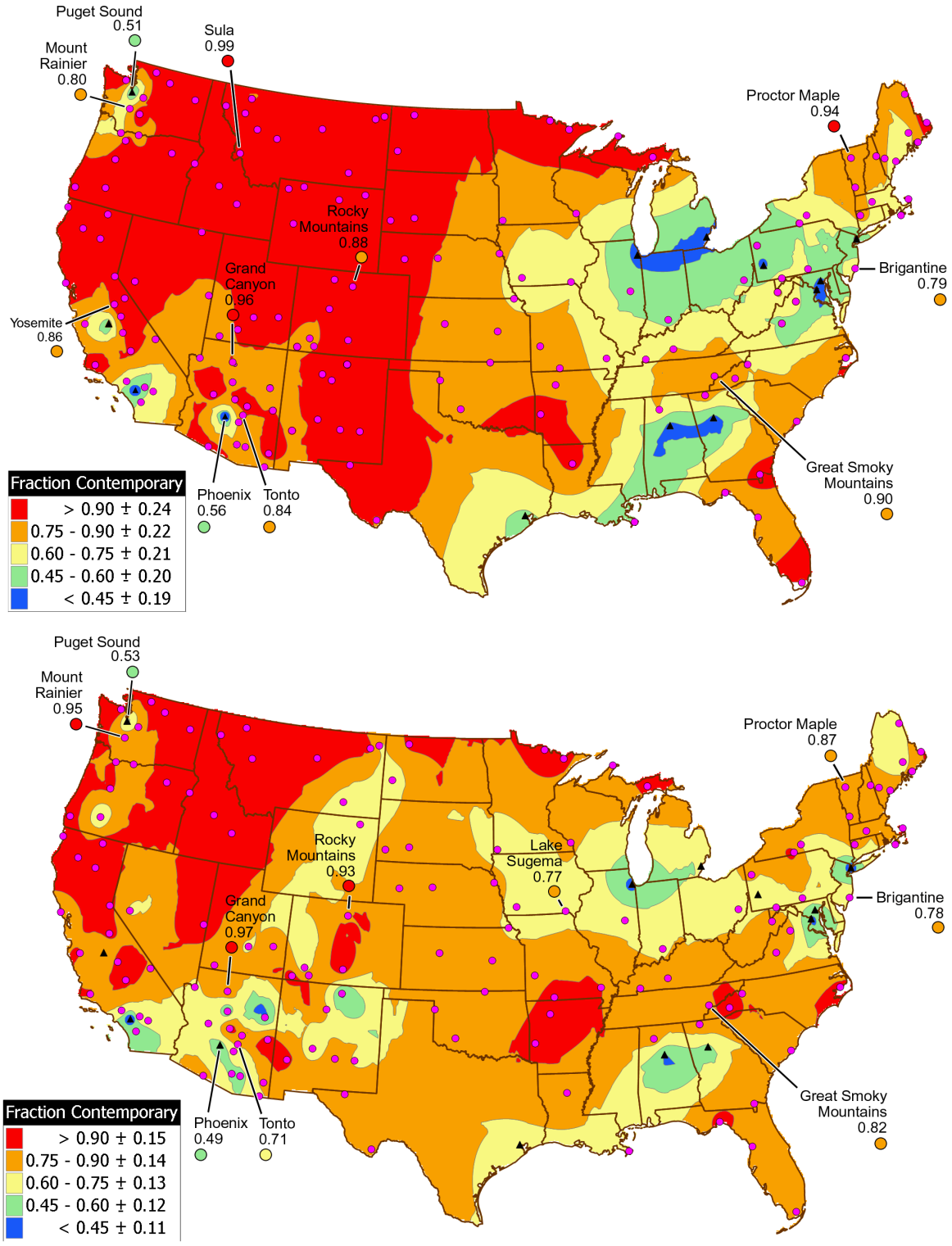

Figure 12. The average fraction contemporary carbon of fine particulate carbon for the summer (top) and winter (bottom) estimated from the December 2004 to February 2006 IMPROVE carbon data. The circles are rural IMPROVE sites and triangles urban IMPROVE sites. The measured fraction contemporary carbon at the twelve sites used in this study is also indicated on the maps. The data are spatially interpolated using a Kriging algorithm to help visualize spatial patterns in the data.

Table 1. Radiocarbon monitoring sites and the median total carbon (TC) concentrations and elemental carbon (EC) to total carbon ratios from collocated IMPROVE monitoring sites for the 2000 through 2004 time period and for each carbon isotope sampling period. The values in parentheses are the median absolute difference (MAD) of the distribution. Bold values are more than 1 MAD from the 2000-2004 median TC or EC/TC.

			2000 - 2004				**Carbon Isotope Sampling Periods**			
			TC (µg/m^3)		**EC/TC**		**TC (µg/m^3)**		**EC/TC**	
Site Name	**Code**	**Setting**	**Summer**	**Winter**	**Summer**	**Winter**	**Summer**	**Winter**	**Summer**	**Winter**
[1]Brigantine, NJ	BRIG	near urban	2.4 (0.87)	2.0 (0.82)	0.18 (0.04)	0.26 (0.03)	2.0 (0.67)	2.0 (0.63)	0.16 (0.03)	0.25 (0.03)
[1]Proctor Maple, VT	PMRF	Rural	1.8 (0.78)	1.1 (0.4)	0.15 (0.03)	0.2 (0.03)	1.8 (0.56)	0.85 (0.33)	0.16 (0.03)	0.22 (0.04)
[1]Great Smoky Mtn, TN	GRSM	Rural	2.3 (0.62)	1.4 (0.43)	0.16 (0.03)	0.21 (0.03)	2.1 (0.46)	1.7 (0.61)	0.14 (0.02)	0.22 (0.03)
[3]Lake Sugema, IA	LASU	near urban	1.8 (0.6)	1.2 (0.36)	0.19 (0.03)	0.2 (0.04)		1.3 (0.31)		**0.27 (0.04)**
[1]Mount Rainier, WA	MORA	near urban	1.8 (0.93)	0.58 (0.38)	0.2 (0.04)	0.2 (0.04)	1.9 (1.1)	**1.3 (0.93)**	0.16 (0.03)	0.23 (0.04)
[1]Puget Sound, WA	PUSO	Urban	2.2 (0.91)	3.7 (1.7)	0.28 (0.07)	0.29 (0.06)	2.4 (1.1)	4.2 (1.6)	0.28 (0.06)	0.32 (0.04)
[2]Grand Canyon, AZ	GRCA	Rural	0.81 (0.27)	0.23 (0.1)	0.14 (0.03)	0.22 (0.06)	0.78 (0.32)	0.2 (0.11)	0.16 (0.04)	0.22 (0.07)
[2]Rocky Mountain, CO	ROMO	Rural	1.4 (0.43)	0.28 (0.11)	0.13 (0.02)	0.17 (0.06)	1.3 (0.57)	0.22 (0.07)	0.15 (0.02)	0.14 (0.05)
[4]Sula, MT	SULA	Rural	1.7 (0.7)	0.27 (0.11)	0.09 (0.02)	0.16 (0.04)	1.2 (0.55)		**0.12 (0.02)**	
[2]Tonto, AZ	TONT	near urban	1.1 (0.3)	0.78 (0.22)	0.13 (0.03)	0.25 (0.05)	1.0 (0.27)	0.71 (0.26)	**0.17 (0.03)**	0.27 (0.04)
[2]Phoenix, AZ	PHOE	Urban	2.2 (.47)	6.9 (3.1)	0.24 (0.04)	0.25 (0.06)	2.3 (0.64)	7.3 (3.0)	0.25 (0.05)	**0.35 (0.04)**
[5]Yosemite, CA	YOSE	Rural	2.1 (.78)	0.33 (0.18)	0.12 (0.02)	0.16 (0.04)	**3.8 (1.5)**		0.1 (0.03)	

[1]Radiocarbon samples collected from 6/2004 – 8/2004 and 12/2004 – 2/2005
[2]Radiocarbon samples collected from 6/2005 – 8/2005 and 12/2005 – 2/2006
[3]Radiocarbon samples collected from 12/2005 – 2/2006
[4]Radiocarbon samples reported for 6/2005 – 8/2005
[5]Radiocarbon samples collected from 7/2002 – 8/2002

Table 2. The summer and winter characteristic EC/TC ratios for contemporary and fossil carbon.

	Summer			Winter		
	EC/TC	Standard Error	95% Confidence Interval	EC/TC	Standard Error	95% Confidence Interval
Contemporary Carbon	0.12	0.039	0.024	0.19	0.0095	0.022
Fossil Carbon	0.35	0.011	0.088	0.46	0.028	0.066

Table 3. Summary of primary EC/TC ratios from mobile sources complied by *Gillies and Gertler* [2000].

	Number of profiles	Mean	Standard Deviation	Minimum	Maximum
[a]**Light Duty Gas Vehicle**	109	0.34	0.22	0.02	0.94
[a]**Diesel**	39	0.61	0.25	0.01	0.91
[b,c]**Mixed Ambient samples**	64	0.40	0.14	0.1	0.79

[a] Included data from SPECIATE, DRI, CE-CERT and NFRAQS
[b] Included data from DRI

Table 4. Summary of primary EC/TC ratios from biogenic (contemporary) combustion sources.

	EC/TC	Standard Deviation	Minimum	Maximum
SPECIATE - Composite Values				
Residential wood combustion	0.21	0.10	0.056	0.46
Slash burning	0.14	0.088	0.018	0.34
Agricultural Field burning	0.14	0.047	0.14	0.23
Forest prescribed burning - broadcast conifer	0.096	--	--	--
Meat cooking	0	--	--	--
Chow et al., [2004]				
Vegetation burning	0.13	0.068	0.073	0.25
Meat cooking	0.089	0.066	0.034	0.18
Reid et al., [2005]				
Mixed vegetation burning	0.14	0.1	0.04	0.38
Average	0.12			
Range	0 - 0.21			

[1]The EC/TC ratios are the reported composite values. The standard deviation, minimum and maximum EC/TC ratios are derived from the reported results from individual studies in the SPECIATE database.

Table 5. EC/TC ratios EC/TC edges.

Percentile	90th	82 th - 98 th	10 th	2nd - 18th
Rural				
Winter	0.32	0.29 - 0.41	0.16	0.11 - 0.18
Summer	0.23	0.2 - 0.3	0.07	0.04 - 0.09
Urban				
Winter	0.44	0.4 - 0.5	0.24	0.17 - 0.26
Summer	0.41	0.37 - 0.48	0.18	0.11 - 0.21

Table 6. Estimate of the contribution of secondary organic carbon to the particulate fossil and contemporary fractions. Errors were estimated by propagating the characteristic EC/TC standard errors reported in Table 2.

		Primary (%)	Secondary (%)
SOC / TC	**Contemporary**	64 ± 6.4	36 ± 6.4
	Fossil	77 ± 10	23 ± 10
SOC / OC	**Contemporary**	59 ± 7.3	41 ± 7.3
	Fossil	64 ± 15	36 ± 15